

Non-holomorphic A_4 modular invariance for fermion masses and mixing in $SU(5)$ GUT

Mohamed Amin Loualidi,^{1,*} Mohamed Miskaoui,^{2,†} and Salah Nasri^{1,‡}

¹*Department of physics, United Arab Emirates University, Al-Ain, UAE*

²*Department of physics, Faculty of Science, Mohammed V University in Rabat, 10090 Rabat, Morocco*

Addressing the fermion flavor structures using modular invariance is a challenging task in the framework of quark-lepton unification. Building on recent applications of modular symmetry in non-supersymmetric models, we propose the first renormalizable $SU(5)$ grand unified theory incorporating level 3 non-holomorphic modular symmetry, $\Gamma_3 \simeq A_4$. This framework constrains Yukawa couplings to polyharmonic Maass forms, significantly reducing the number of free parameters while enhancing the predictive power of the models. We present a comprehensive analysis of fermion masses and mixing while tackling key GUT queries such as gauge coupling unification and proton decay. Beyond the minimal $SU(5)$ framework, the Higgs sector incorporates the 45_H dimensional Higgs field crucial in differentiating the masses of down quarks and charged leptons, and the fermion sector is extended with three right-handed neutrinos enabling neutrino masses via the type-I see-saw mechanism. We analyze two benchmark models with distinct modular weight and A_4 charge assignments. The predicted effective Majorana mass $m_{\beta\beta}$ values align with current neutrinoless double-beta decay experiments, and the effective neutrino mass m_β is within the reach of future beta decay searches. The predicted sum of neutrino masses, $\sum m_i$, satisfies the upper bound set by recent cosmological observations. The gauge coupling unification is achieved through a light scalar triplet $\phi_3 \sim (3, 3, -1/3)$ and a scalar octet $\phi_5 \sim (8, 2, 1/2)$ belonging to the 45_H Higgs, while proton decay constraints require a highly suppressed Yukawa couplings.

I. INTRODUCTION

The quest to understand the origins of fermion masses and their mixing remains a central challenge in particle physics. The distinct mass hierarchies and mixing behaviors observed in the lepton and quark sectors suggest that new physics may be at play, especially with the discovery of neutrino oscillations pointing to physics beyond the standard model (SM) [1, 2]. In particular, unlike quarks where mixing angles are small, neutrino experiments have revealed that two angles in the Pontecorvo-Maki-Nakagawa-Sakata (PMNS) matrix are significantly large [3]. Furthermore, while charge conjugation and parity (CP) symmetry violation is well established in the quark sector—first observed in kaon decays in the 1960s [4]—the idea of CP violation in the lepton sector remains an intriguing possibility yet to be experimentally confirmed. Meanwhile, quark and charged lepton masses originate from their Yukawa interactions with the Higgs field, but the SM offers no explanation for the values of these couplings, leaving them as free parameters determined only by experiment. Additionally, the SM provides no underlying reason for the specific charge assignments of particles or the cancellation of anomalies. Given all these factors, and the fact that the renormalization group (RG) evolution of the three gauge couplings in the SM shows a tendency toward unification at a high energy scale, suggest the need for a more predictive and unified theory. One approach to addressing these open questions is to explore symmetries beyond the gauge symmetry of the SM. In particular, non-Abelian discrete symmetries, which act on different generations of matter particles, naturally lead to large lepton mixing angles. This provides a structured framework for reproducing certain known lepton mixing patterns. For recent reviews on this topic, see Refs. [5–8]. Grand Unified Theories (GUTs) [9–14], on the other hand, unify quarks and leptons within the same multiplets, offering an explanation for the charge quantization and anomaly cancellation while reducing the number of free parameters.

Although combining a non-Abelian symmetry with a GUT appears to be the ideal framework for addressing the shortcomings of the SM, both approaches come with their own challenges and complexities. In flavor model building, introducing a non-Abelian symmetry necessitates breaking it at some stage, which requires additional degrees of freedom in the form of scalar fields known as flavons. These flavons dictate the dynamics of symmetry breaking by requiring intricate vacuum alignments along different directions in flavor space across different fermion sectors. Thus, constructing a viable flavon potential becomes highly complex, often involving the introduction of additional

*Electronic address: ma.loualidi@uaeu.ac.ae

†Electronic address: m.miskaoui@gmail.com

‡Electronic address: snasri@uaeu.ac.ae, salah.nasri@cern.ch

discrete abelian groups to eliminate unwanted operators and ensure the correct vacuum alignment. This complexity in both symmetry breaking and flavon potential construction makes these models difficult to manage, ultimately limiting their simplicity and predictivity. On the other hand, GUTs in their minimal realizations inherently impose degeneracy among fermion masses across different sectors, conflicting with experimental observations. Furthermore, they fail to achieve gauge coupling unification (GCU) without violating proton decay bounds set by Super-Kamiokande [15]. Focusing on the Georgi-Glashow $SU(5)$ model, which embeds the SM gauge group $G_{SM} = SU(3)_C \times SU(2)_L \times U(1)_Y$ within a simple Lie group, this GCU issue is naturally resolved in its supersymmetric extension (SUSY $SU(5)$) [16, 17]. There, the contributions of superpartners to the RG running drive GCU at $\mathcal{O}(10^{16})$ GeV [18–21]. However, the lack of experimental confirmation of low-energy SUSY at current collider limits challenges its viability, motivating renewed interest in alternative scenarios, with non-supersymmetric GUTs as a promising alternative.

To address the fermion flavor structure without the complications of flavon vacuum alignment, modular invariance has been proposed as a flavor symmetry, offering a promising direction for flavor model building [22]. This approach first emerged in specific string compactifications [23–25], where Yukawa couplings are described as modular forms, which are holomorphic functions of a complex scalar field τ , known as the modulus. SUSY naturally provides a framework for constructing such models, in which the modulus acquires a vacuum expectation value (VEV), serving as the sole source of flavor symmetry breaking. Consequently, the introduction of flavons becomes unnecessary, thereby eliminating the associated vacuum alignment problem. In this framework, the superpotential must be invariant under the modular group $\Gamma = SL(2, \mathbb{Z})$ or its projective counterpart, the inhomogeneous modular group $PSL(2, \mathbb{Z})$, defined as the quotient of $SL(2, \mathbb{Z})$ by its center. Although these modular groups are infinite, considering the quotient of $PSL(2, \mathbb{Z})$ by its principal congruence subgroups, $\bar{\Gamma}(N)$, results in finite modular groups¹ $\Gamma_N = PSL(2, \mathbb{Z})/\bar{\Gamma}(N)$ [29]. For $N \leq 5$, these finite modular groups correspond to the well-known non-Abelian discrete symmetries: $\Gamma_2 \simeq S_3$, $\Gamma_3 \simeq A_4$, $\Gamma_4 \simeq S_4$, and $\Gamma_5 \simeq A_5$. Accordingly, both matter fields and the Yukawa couplings transform as irreducible representations of Γ_N . For a comprehensive overview of modular flavor symmetries, see Refs. [30, 31]. As mentioned earlier, low-energy SUSY remains beyond experimental reach, making it imperative to investigate alternative frameworks such as modular invariance without SUSY. A significant breakthrough in this regard was presented in Ref. [32], where modular flavor symmetry was successfully integrated into the lepton sector in a non-SUSY setting. The groundwork for this approach was laid in Ref. [33], where the authors proposed that automorphic forms could enable model-building independent of SUSY by replacing the holomorphicity constraint with a harmonic condition. This led to the replacement of Yukawa couplings, traditionally represented as modular forms, with polyharmonic Maaß forms, which incorporate a non-holomorphic component. As a result, these structures now serve as the fundamental mathematical framework governing flavor symmetries in non-SUSY models. So far, only a few studies have applied this novel approach to flavor model building [34–39]. However, no research has explored its application to quark-lepton unification, which remains a challenging task within the framework of modular symmetry without SUSY.

In this paper, we present the first modular-invariant $\Gamma_3 \cong A_4$ flavor model within a non-SUSY² $SU(5)$ GUT. We investigate its implications for fermion masses and mixing in both the quark and lepton sectors, addressing key challenges of the minimal non-SUSY $SU(5)$ model, such as the failure of GCU and the issue of identical Yukawa couplings for down-type quarks and charged leptons. To resolve these limitations, we extend the Higgs sector by introducing a 45-dimensional Higgs representation, enabling the differentiation of down-type quark and charged lepton masses. Additionally, we incorporate three right-handed neutrinos in the fermion sector to generate neutrino masses via the type-I seesaw mechanism [63–67]. Given the broad flexibility in assigning A_4 representations and modular weights to different fields, we impose theoretical constraints to systematically reduce the model space while maintaining consistency and achieving an optimal fit to experimental data. To simplify the scalar sector, all scalar multiplets are assumed to transform trivially under A_4 with zero modular weight. We further restrict our analysis to level-3 polyharmonic Maaß forms with even modular weights in the range $-4 \leq k_Y \leq 6$. Within this framework, we propose two benchmark renormalizable models, distinguished by the A_4 assignments and modular weights of the right-handed neutrinos and the three generations of matter fields in the conjugate $\bar{5}_{F_i}$ representations. In contrast, the 10_{F_i} matter fields share identical A_4 and modular weight charges in both models. Through a numerical analysis, we determine

¹ An early effort to link ordinary non-Abelian discrete symmetries with the modular group in flavor model building was introduced in Ref. [26], where an A_4 neutrino model was constructed, exploring the origin of the A_4 group as a subgroup of the modular group. Other early studies investigating known neutrino mixing patterns through the modular group $PSL(2, \mathbb{Z})$ were proposed in Refs. [27, 28]. One such approach fixed $\mathbb{Z} = 5$, showing that $PSL(2, 5)$ is isomorphic to the icosahedral group A_5 . Furthermore, the group $PSL(2, 7)$ was studied, highlighting its connection to the non-Abelian S_4 group, which appears as one of its maximal subgroups.

² In the framework of the ordinary SUSY $SU(5)$ GUT in four dimensions, flavor models have been developed using various conventional non-Abelian symmetry groups, including S_4 [40–44] and its subgroups A_4 [45–51], S_3 [52], and D_4 [53–55]. In addition, modular symmetries have been explored in the context of Γ_4 [56–58], Γ_3 [59, 60], and Γ_2 [61, 62]. This list is not exhaustive, as it does not account for variations of the $SU(5)$ model or extensions to larger symmetry groups beyond S_4 .

the best-fit values of the free parameter, including the modulus τ , ensuring consistency with experimental observables in both the quark and lepton sectors. Our results indicate that the normal mass ordering (NO) is favored over the inverted ordering (IO) in benchmark model I, while both mass orderings remain viable in benchmark model II. We provide predictions for key neutrino parameters, including the sum of neutrino masses $\sum m_i$, the effective neutrino mass m_β , the Majorana effective mass $m_{\beta\beta}$, and the CP -violating phases. Notably, the atmospheric mixing angle aligns with experimental data only in the NO scenario, with model I favoring the higher octant and model II the lower octant. The predicted $m_{\beta\beta}$ values agree with current neutrinoless double-beta decay constraints, while m_β remains below present experimental sensitivity but could be tested in future beta decay experiments. Similarly, the predicted sum of neutrino masses, $\sum m_i$, satisfies the upper bound set by recent cosmological observations. In the quark sector, predicted mass ratios and mixing angles at the GUT scale are consistent with experimental data across all models. Moreover, we investigated the role of the 45_H Higgs representation in realizing GCU through threshold corrections induced by its light scalar components. In a scenario where the light spectrum contains a color-triplet scalar ϕ_3 and a color-octet scalar ϕ_5 , unification must occur at a sufficiently high scale to suppress proton decay mediated by gauge bosons. Meanwhile, proton decay via the light Higgs triplet ϕ_3 is further suppressed by stringent constraints on polyharmonic Maaß forms, whereas decay involving heavier scalar triplets remains negligible due to their GUT-scale masses.

The rest of this paper is organized as follows. Sec. II provides a concise introduction to modular invariance, modular forms, and polyharmonic Maaß forms. In Sec. III, we present two benchmark $SU(5)$ models based on the finite modular group $\Gamma_3 \cong A_4$ and derive the corresponding fermion Yukawa matrices. Sec. IV presents a numerical analysis of these benchmark models for both NO and IO neutrino mass spectra, including predictions for fermion mass ratios, mixing parameters, and key neutrino observables such as $m_{\beta\beta}$, m_β , and $\sum m_i$. In Sec. V, we explore the conditions for the GCU and consider scenarios where the components of the 45 Higgs field exhibit a hierarchical mass spectrum. Additionally, we provide a brief analysis of the contribution of the scalar Higgs triplet from the 45 Higgs field to proton decay. We conclude in Sec. VI. Additional details on the A_4 group and higher-weight polyharmonic Maaß forms at level 3 are provided in the appendix.

II. NON-HOLOMORPHIC MODULAR SYMMETRY

Flavor models based on modular invariance provide a compelling framework for understanding the flavor structure of fermions. In particular, $\mathcal{N} = 1$ supersymmetric modular-invariant models within a bottom-up approach, have been remarkably successful in predicting lepton masses and mixing with only a few free parameters [22]. A key feature of these models is that matter fields in the superpotential transform under the inhomogeneous (or homogeneous) modular group $\bar{\Gamma} = PSL(2, \mathbb{Z})$ ($\Gamma = SL(2, \mathbb{Z})$), which requires that the elements of the Yukawa coupling matrices are modular forms. These forms are holomorphic functions of the modulus τ in the upper half-plane \mathbb{H} , and they transform in specific ways under discrete subgroups of $SL(2, \mathbb{R})$ such as $\bar{\Gamma}$ and Γ . Specifically, Γ is the group of linear fractional transformations acting on τ as follows

$$\tau \rightarrow \gamma\tau = \frac{a\tau + b}{c\tau + d}, \quad \text{where } \gamma = \begin{pmatrix} a & b \\ c & d \end{pmatrix} \in \Gamma \text{ with } ad - bc = 1. \quad (\text{II.1})$$

Notice that the matrices $\pm\gamma$ act in the same way on τ , so it is also common to work with the group³ $PSL(2, \mathbb{Z})$. This group is infinite, non-compact, and is generated by two elements, S and T , given by

$$S = \begin{pmatrix} 0 & 1 \\ -1 & 0 \end{pmatrix}, \quad T = \begin{pmatrix} 1 & 1 \\ 0 & 1 \end{pmatrix}, \quad (\text{II.2})$$

which satisfy the relations $S^2 = (ST)^3 = 1$. Under the action of these generators, S transforms τ as $\tau \rightarrow \frac{-1}{\tau}$, whereas T induces the shift $\tau \rightarrow 1 + \tau$.

In flavor models with modular invariance, finite modular groups with finite-dimensional representations play a fundamental role in constructing a well-defined flavor structure while keeping the number of parameters under control.

³ The difference between Γ and $\bar{\Gamma}$ lies in their structure: Γ is the full modular group, consisting of 2×2 matrices with integer coefficients and unit determinant, while $\bar{\Gamma}$ is the projective special linear group, defined as the quotient of Γ by its center: $\bar{\Gamma} = \Gamma / \{\pm I_2\}$, where I_2 is the identity matrix. This distinction reflects the removal of the overall sign ambiguity in Γ .

To achieve this, chiral superfields and modular forms appearing in the superpotential are assumed to transform under representations of discrete finite modular groups, which are defined as $\Gamma_N = \bar{\Gamma}/\bar{\Gamma}(N)$ for the inhomogeneous modular group and $\Gamma'_N = \Gamma/\Gamma(N)$ for the homogeneous one, where N represents the level of the group. Here, $\Gamma(N)$ denotes the infinite principal congruence subgroups of $SL(2, \mathbb{Z})$. These subgroups act on τ similarly to Γ , but with additional modular congruence conditions defined as

$$\Gamma(N) = \left\{ \begin{pmatrix} a & b \\ c & d \end{pmatrix} \in SL(2, \mathbb{Z}) \left| \begin{pmatrix} a & b \\ c & d \end{pmatrix} \equiv \begin{pmatrix} 1 & 0 \\ 0 & 1 \end{pmatrix} \pmod{N} \right. \right\}. \quad (\text{II.3})$$

For $N = 2, 3, 4, 5$, the finite modular groups Γ_N are isomorphic to the permutation groups S_3 , A_4 , S_4 and A_5 [29], while the groups Γ'_N correspond to the double covers of the respective permutation groups [68]. Given how γ acts on τ in Eq. II.1, a modular form $f(\tau)$ of level N transforms under $\Gamma(N)$ as $f(\gamma\tau) = (c\tau + d)^k f(\tau)$ where k is a positive integer called the modular weight. For a given weight k and level N , the modular forms constitute a finite-dimensional vector space, $M_k(\Gamma(N))$, with dimension $k + 1$. It can be readily shown that this space admits a basis in which a multiplet of modular forms $f_i(\tau)$ transforms according to a unitary representation ρ of the finite group Γ_N [22] as

$$f_i(\gamma\tau) = (c\tau + d)^k \rho_{ij}(\gamma) f_j(\tau), \quad \gamma \in \Gamma_N, \quad (\text{II.4})$$

up to the automorphy factor $(c\tau + d)^k$. For example, consider a trilinear term in the superpotential of the form $\mathcal{W}(\tau, \phi) \supset Y_{ijk}(\tau) \phi^i \phi^j \phi^k$. Here the modular forms $Y_{ijk}(\tau)$ transform in the representation ρ_Y of a finite modular group (Γ_N or Γ'_N) and the superfields ϕ_i transform under the action of the modular group as follows

$$Y_{ijk}(\tau) \xrightarrow{\gamma} Y_{ijk}(\gamma\tau) = (c\tau + d)^{k_Y} \rho_Y(\gamma) Y_{ijk}(\tau), \quad \phi_i \xrightarrow{\gamma} (c\tau + d)^{k_i} \rho_i(\gamma) \phi_i \quad (\text{II.5})$$

The term in $\mathcal{W}(\tau, \phi)$ is modular invariant if the modular weights and the representations in Eq. II.5 satisfy: $k_Y = k_i + k_j + k_k$ and $\rho_Y \otimes \rho_i \otimes \rho_j \otimes \rho_k \supset \mathbf{1}$ where $\mathbf{1}$ is the trivial singlet of Γ_N or Γ'_N . Typically, the interplay between modular invariance and the holomorphic nature of the superpotential restricts the allowed terms, significantly reducing the number of free parameters and yielding highly predictive models.

In the above formulation, SUSY ensures the holomorphic structure of Yukawa couplings as modular forms within the superpotential. However, the absence of experimental evidence for low-energy SUSY casts doubt on its existence, motivating the exploration of modular invariance in non-SUSY models, where the field content is significantly reduced. Indeed, a groundbreaking approach has been developed in Ref. [32] in which modular flavor symmetry was successfully applied to the lepton sector in non-SUSY context. This idea was first proposed in Ref. [33], where the authors suggested that the structure of automorphic forms⁴ could offer a path to constructing models without relying on SUSY by replacing the holomorphicity constraint with the harmonic condition. For a single modulus $\tau = x + iy$, these automorphic forms coincide with harmonic Maaß forms F which, unlike purely holomorphic modular functions, have a non-holomorphic component and satisfy the Laplace equation $\Delta_k F = 0$ where Δ_k is the weight k hyperbolic Laplacian operator defined as

$$\Delta_k = -y^2 \left(\frac{\partial^2}{\partial x^2} + \frac{\partial^2}{\partial y^2} \right) + iky \left(\frac{\partial}{\partial x} + i \frac{\partial}{\partial y} \right) = -4y^2 \frac{\partial}{\partial \tau} \frac{\partial}{\partial \bar{\tau}} + 2iky \frac{\partial}{\partial \bar{\tau}}. \quad (\text{II.6})$$

More generally, one can consider polyharmonic Maaß forms, which satisfy $\Delta_k^m F = 0$ for some positive integer m , with $m = 1$ corresponds to harmonic Maaß forms. Accordingly, polyharmonic Maaß forms of level N have been attributed to the Yukawa couplings in the context of non-SUSY models, effectively replacing modular forms as the key mathematical objects governing flavor structures [32]. In this case, Yukawa couplings satisfy the same automorphy condition as modular forms, with the Laplacian condition replacing holomorphicity

$$Y(\gamma\tau) = (c\tau + d)^k Y(\tau), \quad \Delta_k^m Y(\tau) = 0. \quad (\text{II.7})$$

A key distinction from modular forms is that, in the case of polyharmonic Maaß forms, the weight k is an even integer for Γ_N and an integer for Γ'_N . Moreover, these functions are required to grow at a controlled rate as $\text{Im}(\tau) \rightarrow \infty$ where they satisfy a moderate growth condition[69]: $Y(\tau) = \mathcal{O}(y^\alpha)$ for some $\alpha \in \mathbb{R}$ and which holds at all cusps of $\Gamma(N)$ [71]. When applied to flavor model building, the overall construction remains analogous to the modular forms

⁴ Automorphic forms generalize modular forms by extending their applicability to broader groups and spaces [69, 70].

case. At each given weight and level, polyharmonic Maaß forms form a finite-dimensional space, leading to constraints on the Yukawa interactions. Consequently, only a finite number of fermion mass terms are permitted, ensuring that modular invariance retains its predictive power. To illustrate, consider the inhomogeneous finite modular group Γ_N and the Yukawa interaction: $-\mathcal{L} = Y_{ij}^{k_Y}(\tau) \bar{\Psi}_L^i \Phi \Psi_R^j + h.c.$, where $\Psi_{L,R}$ are matter fields, and Φ denotes the Higgs field. Under a modular transformation $\gamma \in \bar{\Gamma}$, these fields transform as

$$\bar{\Psi}_L \xrightarrow{\gamma} (c\tau + d)^{-k_{\bar{\Psi}}} \rho_{\bar{\Psi}}(\gamma) \bar{\Psi}_L, \quad \Psi_R \xrightarrow{\gamma} (c\tau + d)^{-k_{\Psi}} \rho_{\Psi}(\gamma) \Psi_R, \quad \Phi \xrightarrow{\gamma} (c\tau + d)^{-k_{\Phi}} \rho_{\Phi}(\gamma) \bar{\Psi}_L, \quad (\text{II.8})$$

where $k_{\bar{\Psi}}$, k_{Ψ} , k_{Φ} are integer modular weights, and $\rho_{\bar{\Psi}}$, ρ_{Ψ} , ρ_{Φ} are irreducible representations of Γ_N . Modular invariance requires that the coupling $Y_{ij}(\tau)$ is a multiplet of even integer weight k_Y and level N polyharmonic Maaß forms that transforms in a representation ρ_Y of Γ_N as

$$Y^{k_Y}(\tau) \xrightarrow{\gamma} Y^{k_Y}(\gamma\tau) = (c\tau + d)^{k_Y} \rho_Y(\gamma) Y^{k_Y}(\tau) \quad (\text{II.9})$$

where the modular weights and representations must satisfy $k_Y = k_{\bar{\Psi}} + k_{\Psi} + k_{\Phi}$ and $\rho_Y \otimes \rho_{\bar{\Psi}} \otimes \rho_{\Psi} \otimes \rho_{\Phi} \supset \mathbf{1}$.

In this work, We focus on the level $N = 3$ polyharmonic Maaß forms which can be grouped into multiplets of $\Gamma_3 \simeq A_4$. These forms admit an expansion as a Fourier series given by [32]

$$Y(\tau) = \sum_{n \in \frac{1}{N}\mathbb{Z}, n \geq 0} c^+(n) q^n + c^-(0) y^{1-k} + \sum_{n \in \frac{1}{N}\mathbb{Z}, n < 0} c^-(n) \Gamma(1-k, -4\pi n y) q^n, \quad q \equiv e^{2\pi i \tau} \quad (\text{II.10})$$

where the coefficients $c^{\pm}(n)$ and $c^{\pm}(0)$ are constants and $\Gamma(x, y)$ is the incomplete gamma function defined as

$$\Gamma(x, y) = \int_y^{+\infty} e^{-t} t^{x-1} dt \quad (\text{II.11})$$

The expressions of the polyharmonic Maaß forms multiplets of level 3 are given in the Appendix.

III. IMPLEMENTING THE NON-HOLOMORPHIC A_4 GROUP IN $SU(5)$ GUT

In the minimal $SU(5)$ GUT model, the SM fermions are embedded into two irreducible representations: $\bar{5}_{Fi}$ and 10_{Fi} , where $i = 1, 2, 3$ labels the three generations. For a single generation, the fields in $\bar{5}_{F1}$ consist of the charge-conjugate right-handed down-type quark d^c and the left-handed lepton doublet $L = (\nu_L, e_L)$, while 10_{F1} contains the charge-conjugate right-handed up-type quark u^c , the charge-conjugate right-handed charged lepton e^c , and the left-handed quark doublet $Q_L = (u_L, d_L)$. The Higgs sector includes a 24-dimensional adjoint Higgs field H_{24} , responsible for breaking $SU(5)$ down to the SM gauge group, and a fundamental five-dimensional Higgs field 5_H , which contains both a color triplet scalar T and the usual SM Higgs doublet H ; $5_H \equiv H_5 = (T, H)$. Omitting the $SU(5)$ and Lorentz indices, the Yukawa Lagrangian of the model is given by

$$\mathcal{L}_Y = Y_{\bar{5}}^{ij} 10_{Fi} \bar{5}_{Fj} 5_H^* + Y_{10}^{ij} 10_{Fi} 10_{Fj} 5_H + h.c.. \quad (\text{III.12})$$

By decomposing these terms into their SM components, we identify $Y_{\bar{5}}^{ij}$ as encoding the Yukawa couplings for down-type quarks (Y_d^{ij}) and charged leptons (Y_e^{ij}), while Y_{10}^{ij} governs the up-type quark Yukawa interactions (Y_u^{ij}). When the Higgs doublet acquires a VEV at the electroweak scale, it predicts the mass relations $m_e = m_d$, $m_{\mu} = m_s$, and $m_{\tau} = m_b$. While the third-generation relation is reasonable, those for the first two generations conflict with experimental data, where the observed mass ratios are $m_s/m_d \sim 20$ and $m_{\mu}/m_e \sim 200$ [3]. Nearly fifty years ago, Georgi and Jarlskog [72] proposed the first remedy for this issue. They demonstrated that the predicted mass relations could be altered through the application of group-theoretical Clebsch-Gordan (CG) factors, suggesting the need for a more abundant Higgs structure than what the minimal $SU(5)$ model offered. Specifically, they introduced an additional Higgs field, 45_H , transforming in the 45-dimensional representation. This modification introduced an extra term in the Lagrangian given by $Y_{45}^{ij} 10_{Fi} \bar{5}_{Fj} 45_H^*$, where the VEV of this new Higgs is expressed as

$$\langle (H_{45})_{\beta}^{\alpha 5} \rangle = v_{45} (\delta_{\alpha}^{\beta} - 4\delta_4^{\alpha} \delta_{\beta}^4) \quad \text{with} \quad \alpha, \beta = 1, \dots, 4 \quad (\text{III.13})$$

This structure plays a crucial role in differentiating between the masses of charged leptons and down quarks belonging to the first two generations. This distinction arises from the relative factor of -3 in the component $\langle (H_{45})_5^{45} \rangle = -3v_{45}$. Beyond its role in fermion mass generation, the scalar components of 45_H can contribute to gauge coupling unification when some of them acquire masses below M_{GUT} . In such case, these light states

remain active in the renormalization group equations (RGEs) at intermediate scales, affecting the beta functions and modifying the running of gauge couplings. Their contribution can lead to threshold corrections that shift the unification scale and improve the consistency of gauge coupling unification within the model.

We now analyze the modular-invariant $SU(5) \times A_4$ GUT in a renormalizable non-supersymmetric framework, where the minimal $SU(5)$ model is extended with a **45**-dimensional Higgs, as motivated earlier, along with three right-handed neutrinos, $N_{1,2,3}^c$, to account for neutrino masses and mixings by employing the type-I seesaw mechanism. We introduce two benchmark models, each characterized by distinct modular weights and A_4 charge assignments for the various fields involved. In general, a renormalizable Yukawa Lagrangian that respects modular invariance can be formulated as

$$\begin{aligned} \mathcal{L}_Y^{\Gamma_3} = & \sum_{(r \otimes r')_p} \left\{ a_p \left[(T_i T_j H_5)_r Y_{r'}^{(k_{T_i} + k_{T_j} + k_{H_5})}(\tau) \right]_1 + b_p \left[(T_i \bar{F}_j H_5^*)_r Y_{r'}^{(k_{T_i} + k_{\bar{F}_j} + k_{H_5^*})}(\tau) \right]_1 \right. \\ & + b'_p \left[(T_i \bar{F}_j H_{45}^*)_r Y_{r'}^{(k_{T_i} + k_{\bar{F}_j} + k_{H_{45}^*})}(\tau) \right]_1 + c_p \left[(\bar{F}_i N_j^c H_5)_r Y_{r'}^{(k_{\bar{F}_i} + k_{N_j^c} + k_{H_5})}(\tau) \right]_1 \\ & \left. + c'_p \Lambda_p \left[(N_i^c N_j^c)_r Y_{r'}^{(k_{N_i^c} + k_{N_j^c})}(\tau) \right]_1 \right\} + h.c., \end{aligned} \quad (\text{III.14})$$

where the tensor products $(r \otimes r')_p$ encompass all possible combinations that yield the trivial singlet of A_4 (see Eqs. A.3 in the Appendix). The index $p = 1, 2, 3, \dots$ enumerates the distinct A_4 -invariant coupling terms. For instance, consider an A_4 triplet $10_{F_i} \equiv T_i = (T_1, T_2, T_3)^T$ with weight 2 and an A_4 trivial singlet $5_H \equiv H_5$ with weight 0. For the first term in the above Yukawa Lagrangian, the number of invariant terms is determined by the possible weights for the polyharmonic Maaß forms that can be constructed. In this example, there are four such terms ($p = 1, 2, 3, 4$) according to Eqs. A.5-A.18 in the Appendix, given by

$$a_1(T_i T_j H_5)_1 Y_1^4, \quad a_2(T_i T_j H_5)_1'' Y_1^4, \quad a_3(T_i T_j H_5)_{3_S} Y_3^4, \quad a_4(T_i T_j H_5)_{3_A} Y_3^4. \quad (\text{III.15})$$

These correspond to the singlet and triplet contractions of the tensor product, ensuring that the resulting term remains invariant under A_4 . Here, the antisymmetric contraction $(T_i T_j H_5)_{3_A}$ vanishes because the antisymmetric combination of two identical triplets is zero, and thus $a_4 = 0$. Based on the Lagrangian $\mathcal{L}_Y^{\Gamma_3}$ and the VEVs of H_5 , given by $\langle H_5 \rangle = v_5$, and H_{45} in Eq. III.13, we derive the fermion mass matrices for up-type quarks, down-type quarks, charged leptons, and Dirac neutrinos after electroweak (EW) symmetry breaking, which can be expressed as

$$M_u = Y_{10} v_5, \quad M_d = Y_5 v_5^* + Y_{45} v_{45}^*, \quad M_e = Y_5^T v_5^* - 3Y_{45}^T v_{45}^*, \quad M_D = Y_D v_5 \quad (\text{III.16})$$

In the present framework, light neutrino masses are generated through the type-I seesaw mechanism. The mass matrix for the light neutrinos is expressed as $m_\nu = -M_D^T M_R^{-1} M_D$, where M_R denotes the Majorana mass matrix, and M_D is the Dirac mass matrix defined in Eq. III.16. For a more convenient numerical analysis, the Yukawa mass matrices can be reparametrized after diagonalizing the mass matrices, using the VEV of the SM Higgs doublet. Due to the presence of 45_H , this VEV arises from the mixing of the Higgs doublets $H \in H_5$ and $H' \in H_{45}$, leading to $v^2 = v_5^2 + v_{45}^2 = (246 \text{ GeV})^2$. Thus, we define the rescaled Yukawa matrices as

$$\tilde{Y}_{10} = \frac{v_5}{v} Y_{10}, \quad \tilde{Y}_5 = \frac{v_5}{v} Y_5, \quad \tilde{Y}_{45} = \frac{v_{45}}{v} Y_{45}, \quad \tilde{Y}_D = \frac{v_5}{v} Y_D, \quad (\text{III.17})$$

where the new Yukawa matrices remain proportional to the original ones, and the VEV ratios v_5/v and v_{45}/v can be absorbed into the coupling constants of each matrix. Accordingly, the mass matrices in Eq. III.16 are rewritten as follows

$$M_u = \tilde{Y}_{10} v, \quad M_d = (\tilde{Y}_5 + \tilde{Y}_{45}) v, \quad M_e = (\tilde{Y}_5 - 3\tilde{Y}_{45})^T v, \quad M_D = \tilde{Y}_D v. \quad (\text{III.18})$$

The flexibility in assigning A_4 representations and modular weights to different fields results in a variety of possible model constructions. To systematically reduce the number of models to explore, we impose specific constraints that maintain theoretical consistency while ensuring a good fit to experimental data in both the lepton and quark sectors. For simplicity, we assume a trivial scalar sector, where all scalar multiplets transform trivially under A_4 and carry zero modular weight. Additionally, we restrict our analysis to level-3 polyharmonic mass forms with even modular weights in the range $-4 \leq k_Y \leq 6$. Finally, we exclude two limiting cases: (i) all fermions assigned to A_4 singlets and (ii) all fermions assigned to A_4 triplets. The former effectively reduces to a simple Z_3 symmetry, undermining the

motivation for flavor models with non-Abelian discrete groups, which naturally accommodate fermions in doublet and triplet representations for a structured description of neutrino mixing. The latter case, on the other hand, leads to an overconstrained model, making it significantly harder to reconcile with experimental data. With these assumptions in place, we now provide the details of two benchmark $SU(5) \times \Gamma_3$ models.

Model I: In this model, the three generations of matter fields in the **10** representation are assigned to the singlet irreducible representations of A_4 as $(T_1, T_2, T_3) \sim (1'', 1', 1)$, while those in the $\bar{\mathbf{5}}$ representation, and the RH neutrinos, transform as A_4 triplets.

| Model I | T_1 | T_2 | T_3 | \bar{F}_i | N_i^c | H_5^* | H_{45}^* | $Y_1^{(-2)}$ | $Y_3^{(-2)}$ | $Y_3^{(0)}$ | $Y_3^{(2)}$ | $Y_{1'}^{(4)}$ | $Y_1^{(6)}$ |
|---------|----------------|---------------|--------------|--------------------|--------------|--------------------|--------------|--------------|--------------|--------------|--------------|----------------|--------------|
| $SU(5)$ | 10 | 10 | 10 | $\bar{\mathbf{5}}$ | $\mathbf{1}$ | $\bar{\mathbf{5}}$ | 45 | 1 | 1 | 1 | 1 | 1 | 1 |
| A_4 | $\mathbf{1}''$ | $\mathbf{1}'$ | $\mathbf{1}$ | $\mathbf{3}$ | $\mathbf{3}$ | $\mathbf{1}$ | $\mathbf{1}$ | $\mathbf{1}$ | $\mathbf{3}$ | $\mathbf{3}$ | $\mathbf{3}$ | $\mathbf{1}'$ | $\mathbf{1}$ |
| k_I | 4 | 2 | 0 | -2 | 0 | 0 | 0 | -2 | -2 | 0 | 2 | 4 | 6 |

TABLE I: Transformation properties of matter fields, Higgs fields, and polyharmonic Maaß forms in model I under $SU(5) \times A_4$ and their corresponding modular weights.

Table I summarizes the A_4 charge assignments and the modular weights for all fields in the model, along with the polyharmonic Maaß forms ensuring the modular invariance of the Lagrangian. The renormalizable Yukawa interactions, preserving both $SU(5)$ gauge symmetry and the modular group Γ_3 , are given by

$$\begin{aligned}
-\mathcal{L}_Y^I = & a_1(T_1 T_2)_1 Y_1^{(6)} H_5 + a_2(T_1 T_3)_{1''} Y_{1'}^{(4)} H_5 + a_3(T_2 T_2)_{1''} Y_{1'}^{(4)} H_5 + a_4(T_3 T_3)_1 H_5 + b_1(T_1 \bar{F}_j)_3 Y_3^{(2)} H_5^* \\
& + b_2(T_2 \bar{F}_j)_3 Y_3^{(0)} H_5^* + b_3(T_3 \bar{F}_j)_3 Y_3^{(-2)} H_5^* + b'_1(T_1 \bar{F}_j)_3 Y_3^{(2)} H_{45}^* + b'_2(T_2 \bar{F}_j)_3 Y_3^{(0)} H_{45}^* \\
& + b'_3(T_3 \bar{F}_j)_3 Y_3^{(-2)} H_{45}^* + c_1(\bar{F}_i N_j^c)_1 Y_1^{(-2)} H_5 + c_2(\bar{F}_i N_j^c)_3 Y_3^{(-2)} H_5 + c'_1 \Lambda_1 (N_i^c N_j^c)_1 + c'_2 \Lambda_2 (N_i^c N_j^c)_3 Y_3^{(0)} + h.c.
\end{aligned} \quad (\text{III.19})$$

Following the decomposition of the tensor product of the irreducible representations of A_4 (see Appendix), the resulting structure of this Lagrangian gives rise to the following Yukawa matrices

$$\begin{aligned}
Y_{10} &= \begin{pmatrix} 0 & a_1 Y_1^{(6)} & a_2 Y_{1'}^{(4)} \\ a_1 Y_1^{(6)} & a_3 Y_{1'}^{(4)} & 0 \\ a_2 Y_{1'}^{(4)} & 0 & a_4 \end{pmatrix}, \quad Y_{\bar{5}} = \begin{pmatrix} b_1 Y_{3,2}^{(2)} & b_2 Y_{3,3}^{(0)} & b_3 Y_{3,1}^{(-2)} \\ b_1 Y_{3,1}^{(2)} & b_2 Y_{3,2}^{(0)} & b_3 Y_{3,3}^{(-2)} \\ b_1 Y_{3,3}^{(2)} & b_2 Y_{3,1}^{(0)} & b_3 Y_{3,2}^{(-2)} \end{pmatrix}, \\
Y_{45} &= \begin{pmatrix} b'_1 Y_{3,2}^{(2)} & b'_2 Y_{3,3}^{(0)} & b'_3 Y_{3,1}^{(-2)} \\ b'_1 Y_{3,1}^{(2)} & b'_2 Y_{3,2}^{(0)} & b'_3 Y_{3,3}^{(-2)} \\ b'_1 Y_{3,3}^{(2)} & b'_2 Y_{3,1}^{(0)} & b'_3 Y_{3,2}^{(-2)} \end{pmatrix}, \quad Y_D = \begin{pmatrix} c_1 Y_1^{(-2)} + 2c_2 Y_{3,1}^{(-2)} & 0 & -2c_2 Y_{3,2}^{(-2)} \\ -2c_2 Y_{3,3}^{(-2)} & 2c_2 Y_{3,2}^{(-2)} & c_1 Y_1^{(-2)} \\ 0 & c_1 Y_1^{(-2)} - 2c_2 Y_{3,1}^{(-2)} & 2c_2 Y_{3,3}^{(-2)} \end{pmatrix} \quad (\text{III.20})
\end{aligned}$$

The fermion mass matrices are obtained using the same method employed to derive their expressions in Eq. VII. We then factorize each Yukawa matrix with a coupling constant, allowing us to express the input parameters for our numerical study in terms of overall mass scales, coupling constant ratios, and the complex modulus τ , which is associated with polyharmonic Maaß forms. The phases of the parameters a_3 , b_1 , b_2 , b_3 , b'_1 , c_1 , c_2 , c'_1 are unphysical, while the remaining parameters are complex. This model features three overall mass scales: $a_3 v$ in the up-quark mass matrix, $b_3 v$ in both the down-quark and charged lepton mass matrices, and an additional factor for the neutrino mass matrix, which is discussed below. For the Majorana mass matrix of the RH neutrinos denoted as M_R , it is derived from the last two terms in Eq. III.23. Then, the lightest neutrino masses are generated by the type-I seesaw mechanism where $m_\nu = -M_D^T M_R^{-1} M_D$. Assuming for simplicity that $\Lambda_1 = \Lambda_2 = \Lambda$, the expressions for M_R and M_D for model I are given by

$$M_R = c'_1 \Lambda \begin{pmatrix} 1 + 2\frac{c'_2}{c'_1} Y_{3,1}^{(0)} & -\frac{c'_2}{c'_1} Y_{3,3}^{(0)} & -\frac{c'_2}{c'_1} Y_{3,2}^{(0)} \\ -\frac{c'_2}{c'_1} Y_{3,3}^{(0)} & 2\frac{c'_2}{c'_1} Y_{3,2}^{(0)} & 1 - \frac{c'_2}{c'_1} Y_{3,1}^{(0)} \\ -\frac{c'_2}{c'_1} Y_{3,2}^{(0)} & 1 - \frac{c'_2}{c'_1} Y_{3,1}^{(0)} & 2\frac{c'_2}{c'_1} Y_{3,3}^{(0)} \end{pmatrix}, \quad M_D = c_1 v \begin{pmatrix} Y_1^{(-2)} + 2\frac{c_2}{c_1} Y_{3,1}^{(-2)} & 0 & -2\frac{c_2}{c_1} Y_{3,2}^{(-2)} \\ -2\frac{c_2}{c_1} Y_{3,3}^{(-2)} & 2\frac{c_2}{c_1} Y_{3,2}^{(-2)} & Y_1^{(-2)} \\ 0 & Y_1^{(-2)} - 2\frac{c_2}{c_1} Y_{3,1}^{(-2)} & 2\frac{c_2}{c_1} Y_{3,3}^{(-2)} \end{pmatrix} \quad (\text{III.21})$$

From the type I seesaw formula, $m_\nu = -M_D^T M_R^{-1} M_D$, we obtain an additional overall mass scale given by $(c_1 v)^2 / c'_1 \Lambda$. As a result, model I contains a total of 21 independent real parameters, including both the real and imaginary parts of the modulus τ .

Model II: In this model, the A_4 charge assignments for the matter fields in the 10_{F_i} and $\bar{5}_{F_i}$ representations remain unchanged from Model I. However, the right-handed neutrinos have different assignments, transforming as A_4

singlets with charges $(N_1^c, N_2^c, N_3^c) \sim (1, 1'', 1')$. The weights for T_1, T_2 , and T_3 are the same as in Model I, leading to a similar up-quark mass matrix. In contrast, the different weight of $5F_i$ results in modified mass matrices for charged leptons, down quarks, and neutrino Dirac masses. See Table II for the A_4 charge and weight assignments of all fields, along with the polyharmonic Maaß forms relevant for this model.

| Model II | T_1 | T_2 | T_3 | \bar{F}_i | N_1^c | N_2^c | N_3^c | H_5^* | H_{45}^* | $Y_3^{(-4)}$ | $Y_3^{(-2)}$ | $Y_1^{(4)}$ | $Y_{1'}^{(4)}$ | $Y_1^{(6)}$ |
|----------|----------------|---------------|--------------|--------------|--------------|----------------|---------------|--------------|--------------|--------------|--------------|--------------|----------------|--------------|
| $SU(5)$ | 10 | 10 | 10 | $\bar{5}$ | 1 | 1 | 1 | 5 | 45 | 1 | 1 | 1 | 1 | 1 |
| A_4 | $\mathbf{1}''$ | $\mathbf{1}'$ | $\mathbf{1}$ | $\mathbf{3}$ | $\mathbf{1}$ | $\mathbf{1}''$ | $\mathbf{1}'$ | $\mathbf{1}$ | $\mathbf{1}$ | $\mathbf{3}$ | $\mathbf{3}$ | $\mathbf{1}$ | $\mathbf{1}'$ | $\mathbf{1}$ |
| k_I | 4 | 2 | 0 | -4 | 0 | 2 | 2 | 0 | 0 | -4 | -2 | 4 | 4 | 6 |

TABLE II: Same as Table I but for model II.

Given the requirement of invariance under both the $SU(5)$ and the modular symmetry Γ_3 , the renormalizable Yukawa Lagrangian takes the form

$$\begin{aligned}
-\mathcal{L}_Y^{II} = & a_1(T_1 T_2)_1 Y_1^{(6)} H_5 + a_2(T_1 T_3)_{1''} Y_{1'}^{(4)} H_5 + a_3(T_2 T_2)_{1''} Y_{1'}^{(4)} H_5 + a_4(T_3 T_3)_1 H_5 + b_1 T_1 (\bar{F}_j Y_3^{(0)})_{1'} H_5^* \\
& + b_2 T_2 (\bar{F}_j Y_3^{(-2)})_{1''} H_5^* + b_3 T_3 (\bar{F}_j Y_3^{(-4)})_1 H_5^* + b'_1 T_1 (\bar{F}_j Y_3^{(0)})_{1'} H_{45}^* + b'_2 T_2 (\bar{F}_j Y_3^{(-2)})_{1''} H_{45}^* \\
& + b'_3 T_3 (\bar{F}_j Y_3^{(-4)})_1 H_{45}^* + c_1 (\bar{F}_i N_1^c)_3 Y_3^{(-4)} H_5 + c_2 (\bar{F}_i N_2^c)_3 Y_3^{(-2)} H_5 + c_3 (\bar{F}_i N_3^c)_3 Y_3^{(-2)} H_5 \\
& + c'_1 \Lambda_1 (N_1^c N_1^c)_1 + c'_2 \Lambda_2 (N_2^c N_3^c)_3 Y_{1'}^{(4)} + c'_3 \Lambda_2 (N_3^c N_3^c)_3 Y_{1'}^{(4)} + h.c.
\end{aligned} \tag{III.22}$$

Using the decomposition of the tensor product of A_4 representations from Eq. A.5, we derive the Majorana mass matrix and the Yukawa matrices for this model. We find

$$Y_5 = \begin{pmatrix} b_1 Y_{3,2}^{(0)} & b_2 Y_{3,3}^{(-2)} & b_3 Y_{3,1}^{(-4)} \\ b_1 Y_{3,1}^{(0)} & b_2 Y_{3,2}^{(-2)} & b_3 Y_{3,3}^{(-4)} \\ b_1 Y_{3,3}^{(0)} & b_2 Y_{3,1}^{(-2)} & b_3 Y_{3,2}^{(-4)} \end{pmatrix}, \quad Y_D = \begin{pmatrix} c_1 Y_{3,1}^{(-4)} & c_1 Y_{3,3}^{(-4)} & c_1 Y_{3,2}^{(-4)} \\ c_2 Y_{3,2}^{(-2)} & c_2 Y_{3,1}^{(-2)} & c_2 Y_{3,3}^{(-2)} \\ c_3 Y_{3,3}^{(-2)} & c_3 Y_{3,2}^{(-2)} & c_3 Y_{3,1}^{(-2)} \end{pmatrix}, \quad M_R = c'_1 \Lambda \begin{pmatrix} 1 & 0 & 0 \\ 0 & 0 & \frac{c'_2}{c'_1} Y_1^{(4)} \\ 0 & \frac{c'_2}{c'_1} Y_1^{(4)} & \frac{c'_3}{c'_1} Y_{1'}^{(4)} \end{pmatrix} \tag{III.23}$$

The Yukawa matrix for the up-type quarks, Y_{10} , is the same as the one derived in model I (see Eq. III.20). On the other hand, the Yukawa matrix associated with the 45-dimensional Higgs, Y_{45} , closely resembles Y_5 , except that the couplings b_i are replaced by b'_i . As in model I, the couplings a_3 , b_1 , b_2 , b_3 , b'_1 , c_1 , c_2 , c_3 , c'_1 are unphysical, while the remaining couplings are complex. Consequently, the model contains a total of 24 free parameters. In the following section, we carry out a detailed numerical analysis of the two proposed models, identifying regions in the parameter space that show excellent agreement with experimental data for both the lepton and quark sectors.

IV. NUMERICAL RESULTS

In this section, we provide a detailed numerical analysis of fermion flavor structure predictions for the two benchmark $SU(5) \otimes \Gamma_3$ models introduced earlier. These models differ in their modular weight assignments and the A_4 transformation properties of certain matter fields as described in Tables I and II. Our study employs polyharmonic Maaß forms of level 3, incorporating multiplets with modular weights $k_Y = -4, -2, 0, 2, 4, 6$. The Yukawa matrices, given in Eqs. III.20 and III.23, depend on modulus τ , coupling constant ratios, and mass scales, which govern fermion masses, mixings, and CP violating phases. Our analysis is conducted at the GUT scale, using quark and charged lepton masses and CKM mixing angles from Ref. [73]. For neutrino oscillation parameters, we adopt the latest NuFIT v6.0 global fit, which includes Super-Kamiokande atmospheric data [74]. Therefore, their RGE effects from the low-energy to the GUT scale are not considered. Numerical values for all the parameters can be found in Table III.

| Parameters | $\mu_i \pm 1\sigma$ | Parameters | $\mu_i \pm 1\sigma$ | 3σ ranges |
|------------------------|-------------------------|---|---------------------------------|-------------------------------|
| m_e/m_μ | 0.004737 ± 0.000007 | $\Delta m_{21}^2/10^{-5} eV^2$ | 7.49 ± 0.19 | $6.92 \rightarrow 8.05$ |
| m_μ/m_τ | 0.058823 ± 0.000083 | $\Delta m_{31}^2/10^{-3} eV^2(\text{NO})$ | $2.513^{+0.021}_{-0.019}$ | $2.451 \rightarrow 2.578$ |
| m_u/m_c | 0.001857 ± 0.000629 | $\Delta m_{32}^2/10^{-3} eV^2(\text{IO})$ | -2.484 ± 0.020 | $-2.547 \rightarrow -2.421$ |
| m_c/m_t | 0.003194 ± 0.000098 | $\sin^2 \theta_{12}^l$ | $0.308^{+0.012}_{-0.011}$ | $0.275 \rightarrow 0.345$ |
| m_d/m_s | 0.052827 ± 0.005812 | $\sin^2 \theta_{23}^l(\text{NO})$ | $0.470^{+0.017}_{-0.013}$ | $0.435 \rightarrow 0.585$ |
| m_s/m_b | 0.021710 ± 0.001163 | $\sin^2 \theta_{23}^l(\text{IO})$ | $0.550^{+0.012}_{-0.015}$ | $0.440 \rightarrow 0.584$ |
| θ_{12}^q | 0.2274 ± 0.00052 | $\sin^2 \theta_{13}^l(\text{NO})$ | $0.02215^{+0.00056}_{-0.00058}$ | $0.02030 \rightarrow 0.02388$ |
| θ_{13}^q | 0.0042 ± 0.00017 | $\sin^2 \theta_{13}^l(\text{IO})$ | 0.02231 ± 0.00056 | $0.02060 \rightarrow 0.02409$ |
| θ_{23}^q | 0.0485 ± 0.00070 | $\delta_{CP}^l/^\circ(\text{NO})$ | 212^{+26}_{-41} | $124 \rightarrow 364$ |
| $\delta_{CP}^q/^\circ$ | 69.16 ± 7.89 | $\delta_{CP}^l/^\circ(\text{IO})$ | 274^{+22}_{-25} | $201 \rightarrow 335$ |

TABLE III: Best-fit values and 1σ uncertainties for charged fermion mass ratios, quark mixing angles, and the Dirac CP -violating phase at the GUT scale ($M_{GUT} = 2 \times 10^{16}$ GeV), taken from Ref. [73]. The lepton mixing angles, neutrino mass squared differences, and leptonic CP -violating phase from the latest global fit NuFIT v6.0, including Super-Kamiokande atmospheric data for normal and inverted neutrino mass ordering [74].

The standard parametrization is adopted for both the lepton and quark mixing matrices. The unitary matrix U follows the PDG convention and is given by [3]

$$U = \begin{pmatrix} c_{12}c_{13} & s_{12}c_{13} & s_{13}e^{-i\delta_{CP}} \\ -s_{12}c_{23} - c_{12}s_{13}s_{23}e^{i\delta_{CP}} & c_{12}c_{23} - s_{12}s_{13}s_{23}e^{i\delta_{CP}} & c_{13}s_{23} \\ s_{12}s_{23} - c_{12}s_{13}c_{23}e^{i\delta_{CP}} & -c_{12}s_{23} - s_{12}s_{13}c_{23}e^{i\delta_{CP}} & c_{13}c_{23} \end{pmatrix}. \quad (\text{IV.24})$$

For the PMNS matrix, $\theta_{ij} \equiv \theta_{ij}^l$ and $\delta_{CP} \equiv \delta_{CP}^l$, with an additional diagonal phase matrix $\text{diag}(1, e^{i\alpha_{21}/2}, e^{i\alpha_{31}/2})$ accounting for the Majorana phases. For the CKM matrix, $\theta_{ij} \equiv \theta_{ij}^q$ and $\delta_{CP} \equiv \delta_{CP}^q$. We analyze the predictions of the two benchmark $SU(5) \times \Gamma_3$ models for charged fermion mass ratios, quark-sector mixing, CP violating phases, and neutrino oscillation parameters. The Majorana phases in the PMNS matrix directly impact the phenomenology of neutrino mass constraints. The absolute neutrino mass scale can be probed using three different observables:

(i) Sun of three neutrino masses $\sum m_i$ from cosmological observations: Within the framework of the Λ CDM model, the latest Planck CMB measurements (TT, TE, EE + lowE + lensing) provide an upper bound on the sum of neutrino masses $\sum m_i < 0.24$ eV at 95% confidence level (CL) [75]. When further combined with baryon acoustic oscillation (BAO) data, this constraint tightens to $\sum m_i < 0.12$ eV at 95% CL [75].

(ii) The effective Majorana mass $m_{\beta\beta}$ in neutrinoless double beta decay experiments: This process is a key probe of the Majorana nature of neutrinos. Its decay rate depends on the Majorana CP phases and the effective mass $|m_{\beta\beta}|$ defined as $|m_{\beta\beta}| = |\sum_i U_{ei}^2 m_i|$. KamLAND-Zen experiment sets the most stringent limit on $0\nu\beta\beta$ -decay half-life, which provides an upper bound on $|m_{\beta\beta}|$ given by $|m_{\beta\beta}| < (28 \sim 122)$ meV [76]. Future large-scale $0\nu\beta\beta$ -decay experiments, such as LEGEND-1000 and nEXO [60], aim to improve sensitivity, with LEGEND-1000 targeting $m_{\beta\beta}$ in the range of 9 – 21 meV [77], and nEXO aiming for 4.7 – 20.3 meV [78].

(iii) The effective neutrino mass m_β in beta decay experiments: Tritium beta decay provides a direct probe of the neutrino mass scale by analyzing the electron energy spectrum near its endpoint. The effective anti-electron neutrino mass squared is defined as $m_\beta^2 = \sum_{i=1}^3 |U_{ei}|^2 m_i^2$. The KATRIN collaboration currently constrains $m_\beta < 0.45$ eV [79], with a future sensitivity goal of 0.2 eV [80].

To assess the phenomenological viability of our benchmark models for both NO and IO, we perform a standard χ^2 analysis, with the χ^2 function defined as

$$\chi^2 = \sum_i \left(\frac{Q_i(p) - \mu_i}{\sigma_i} \right)^2, \quad (\text{IV.25})$$

where μ_i and σ_i denote the global best-fit values and corresponding 1σ uncertainties, respectively, for the 16 flavor observables listed in Table III. The quantities $Q_i(p)$ represent the theoretical predictions for these observables, expressed as functions of the free parameters of each model $p = \{\tau, a_i/a_3, b_i/b_3, b'_i/b_3, \dots\}$. The modulus τ is considered as a free

| Parameters | Model I (NO) | Model I (IO) | Model II (NO) | Model II (IO) |
|---------------------------------------|--------------------------|----------------------------|-------------------------------|-------------------------------|
| $Re(\tau)$ | 0.1281 | 0.0103 | 0.0476 | -0.2831 |
| $Im(\tau)$ | 1.6823 | 2.2648 | 1.7104 | 1.6590 |
| a_1/a_3 | $0.1443e^{0.2925\pi i}$ | $0.46934e^{-0.50701\pi i}$ | $1.1834e^{0.9584\pi i}$ | $1.3868e^{0.8950\pi i}$ |
| a_2/a_3 | $7.681e^{0.6975\pi i}$ | $357.094e^{-0.37838\pi i}$ | $228.6683e^{-0.2669\pi i}$ | $249.2469e^{-0.0387\pi i}$ |
| $a_3\nu$ (GeV) | 38.5662 | 68.2266 | 165.9036 | 68.2602 |
| a_4/a_3 | $128.90e^{-0.9322\pi i}$ | $675.274e^{0.28897\pi i}$ | $1398.5939e^{-0.3610\pi i}$ | $1651.0574e^{-0.2782\pi i}$ |
| b_1/b_3 | 1.5381 | 1.3174 | 0.2582 | 0.0521 |
| b_2/b_3 | 100.5243 | -984.3330 | -87.9918 | -10.5364 |
| $b_3\nu$ (GeV) | 57.8613 | 0.0973 | 86.7449 | 166.0648 |
| b'_1/b_3 | 0.5024 | 0.3122 | 0.1273 | 0.0343 |
| b'_2/b_3 | $6.874e^{0.9384\pi i}$ | $97.3373e^{-0.61665\pi i}$ | $97.9927e^{-0.7851\pi i}$ | $35.7346e^{-0.8508\pi i}$ |
| b'_3/b_3 | $0.9314e^{0.9985\pi i}$ | $6.9251e^{-0.30634\pi i}$ | $2.5877e^{0.6506\pi i}$ | $0.9658e^{0.7905\pi i}$ |
| c_2/c_1 | 0.1516 | -9.1 | 722.5162 | 185.3394 |
| c_3/c_1 | --- | --- | -883.9098 | -1014.7310 |
| c'_2/c'_1 | $2.458e^{0.2027\pi i}$ | $0.94975e^{0.00121\pi i}$ | $185442.2760e^{0.3944\pi i}$ | $105888.2838e^{0.4987\pi i}$ |
| c'_3/c'_1 | --- | --- | $216055.8955e^{-0.0428\pi i}$ | $940437.4129e^{-0.0432\pi i}$ |
| $\frac{(c_1\nu)^2}{c'_1\Delta}$ (meV) | 124.1089 | 0.0398 | 4.8530 | 9.1278 |
| m_e/m_μ | 0.004737 | 0.004747 | 0.004736 | 0.004746 |
| m_μ/m_τ | 0.0588 | 0.0588 | 0.0588 | 0.0588 |
| m_1 (meV) | 76.00 | 50.87 | 40.55 | 57.55 |
| m_2 (meV) | 76.49 | 51.60 | 41.46 | 58.20 |
| m_3 (meV) | 91.02 | 13.40 | 64.47 | 30.09 |
| $\sin^2\theta_{12}^l$ | 0.308 | 0.308 | 0.308 | 0.308 |
| $\sin^2\theta_{13}^l$ | 0.02249 | 0.02281 | 0.02217 | 0.02217 |
| $\sin^2\theta_{23}^l$ | 0.5109 | 0.7838 | 0.4536 | 0.6096 |
| δ_{CP}^l/π | 1.599 | 1.475 | 0.522 | 1.467 |
| α_{21}/π | 1.544 | 1.582 | 1.506 | 1.622 |
| α_{31}/π | 1.574 | 0.428 | 0.433 | 1.576 |
| m_β (meV) | 76.53 | 51.54 | 41.52 | 58.16 |
| $m_{\beta\beta}$ (meV) | 131.28 | 45.35 | 40.479 | 56.56 |
| m_u/m_c | 0.001860 | 0.001874 | 0.001856 | 0.001886 |
| m_c/m_t | 0.003191 | 0.003192 | 0.003193 | 0.003353 |
| m_d/m_s | 0.053783 | 0.054773 | 0.052822 | 0.04743 |
| m_s/m_b | 0.02306 | 0.020313 | 0.02171 | 0.02158 |
| θ_{12}^q | 0.2273 | 0.2272 | 0.2274 | 0.2272 |
| θ_{13}^q | 0.0041 | 0.0042 | 0.0042 | 0.0042 |
| θ_{23}^q | 0.04877 | 0.04757 | 0.04851 | 0.04814 |
| $\delta_{CP}^q/^\circ$ | 69.08 | 60.93 | 69.14 | 61.60 |
| χ_l^2 | 0.737883 | 11.384881 | 1.013631 | 0.715045 |
| χ_q^2 | 0.172793 | 0.069399 | 0.000014 | 1.115284 |
| χ_{total}^2 | 0.910676 | 11.888987 | 1.013645 | 1.830329 |

TABLE IV: The best-fit values of the model parameters, along with the corresponding predictions for fermion masses and mixing, are presented for the two benchmark $SU(5) \times \Gamma_3$ models in both NO and IO. The numerical values of the physical observables are summarized in Table III.

parameter where its value varies within the fundamental domain $\mathcal{D} = \{\tau \in \mathbb{C} | Im(\tau) > 0, |Re(\tau)| \leq \frac{1}{2}, |\tau| \geq 1\}$. The total χ^2 can be thought of as the sum of two contributions: χ_l^2 for leptonic observables and χ_q^2 for quark observables. Specifically, χ_l^2 is constructed from charged lepton mass ratios and neutrino oscillation parameters, while χ_q^2 is based on quark mass ratios, quark mixing angles, and the Dirac CP violating phase as listed in Table III.

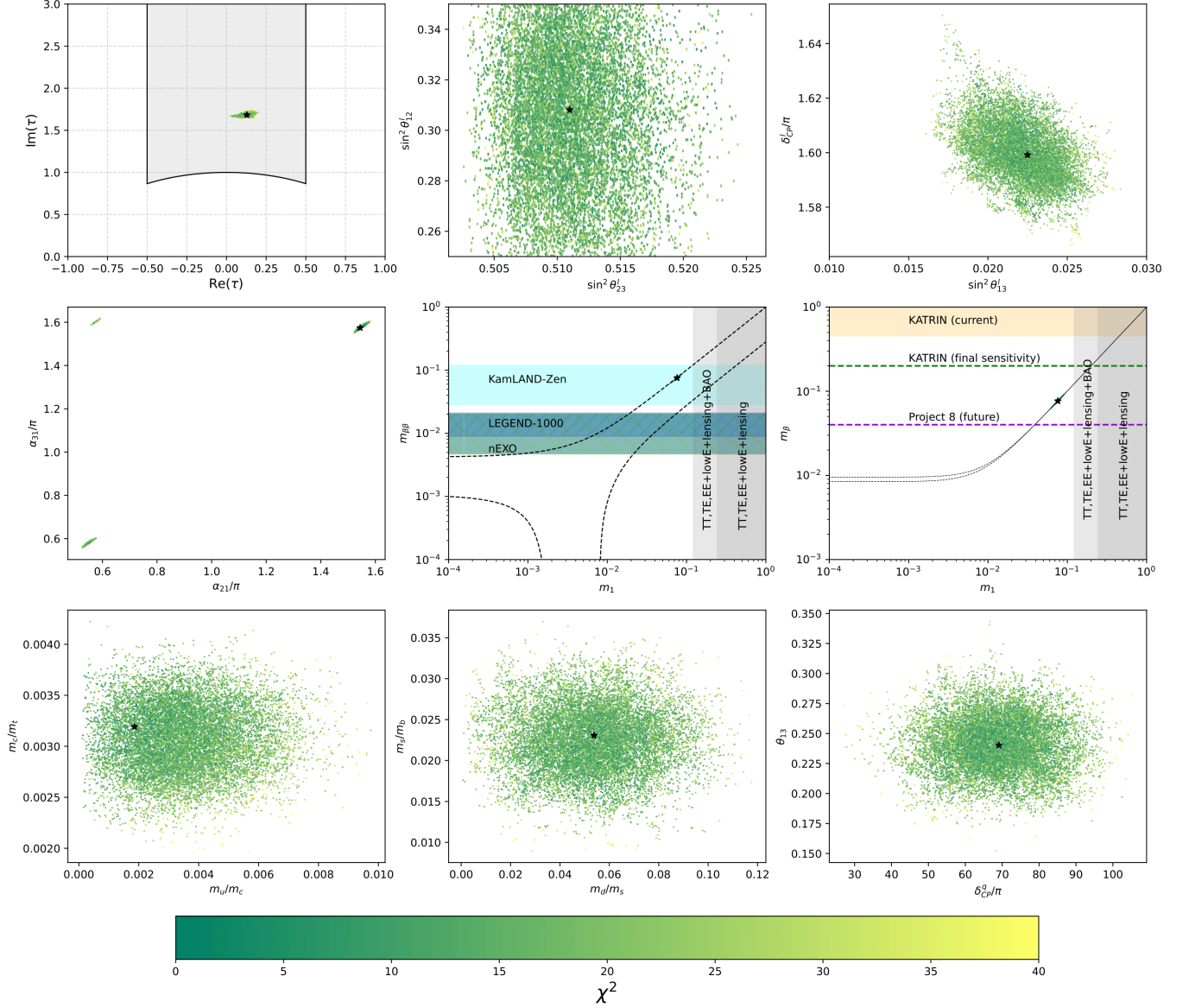


FIG. 1: Allowed parameter space for τ and the predicted correlations among quark and lepton observables in model I for the NO case. The black star represents the best-fit point. The gray-shaded regions the Planck limits on the sum of neutrino masses, $\sum m_i$ [75]. Additionally, the shaded regions in the m_β and $m_{\beta\beta}$ panels correspond to experimental constraints from beta decay and neutrinoless double-beta ($0\nu\beta\beta$) decay experiments.

To determine the masses and mixing angles of quarks and leptons, we apply singular value decomposition to the mass matrices and then compute the total χ^2_{total} . All dimensionless parameters are treated as independent variables, with their magnitudes randomly varied within $[0, 10^4]$, while their phases are varied in the range $[0, 2\pi]$. We numerically minimize the χ^2_{total} function using the **FlavorPy** package [81] to determine the parameter values that best align with experimental data, thereby evaluating the validity of each model⁵. The package utilizes the **lmfit** algorithm for parameter optimization and conducts a Markov Chain Monte Carlo (MCMC) scan around the best-fit point to explore parameter uncertainties. A model is considered phenomenologically viable if it predicts all or nearly all of the 16 observables listed in Table III within their 3σ experimental limits. This requires a sufficiently low χ^2_{total} , and we restrict our analysis to models satisfying $\chi^2_{\text{total}} < 10$.

⁵ A similar procedure was recently employed in Ref. [82] within the context of a SUSY modular flavor model.

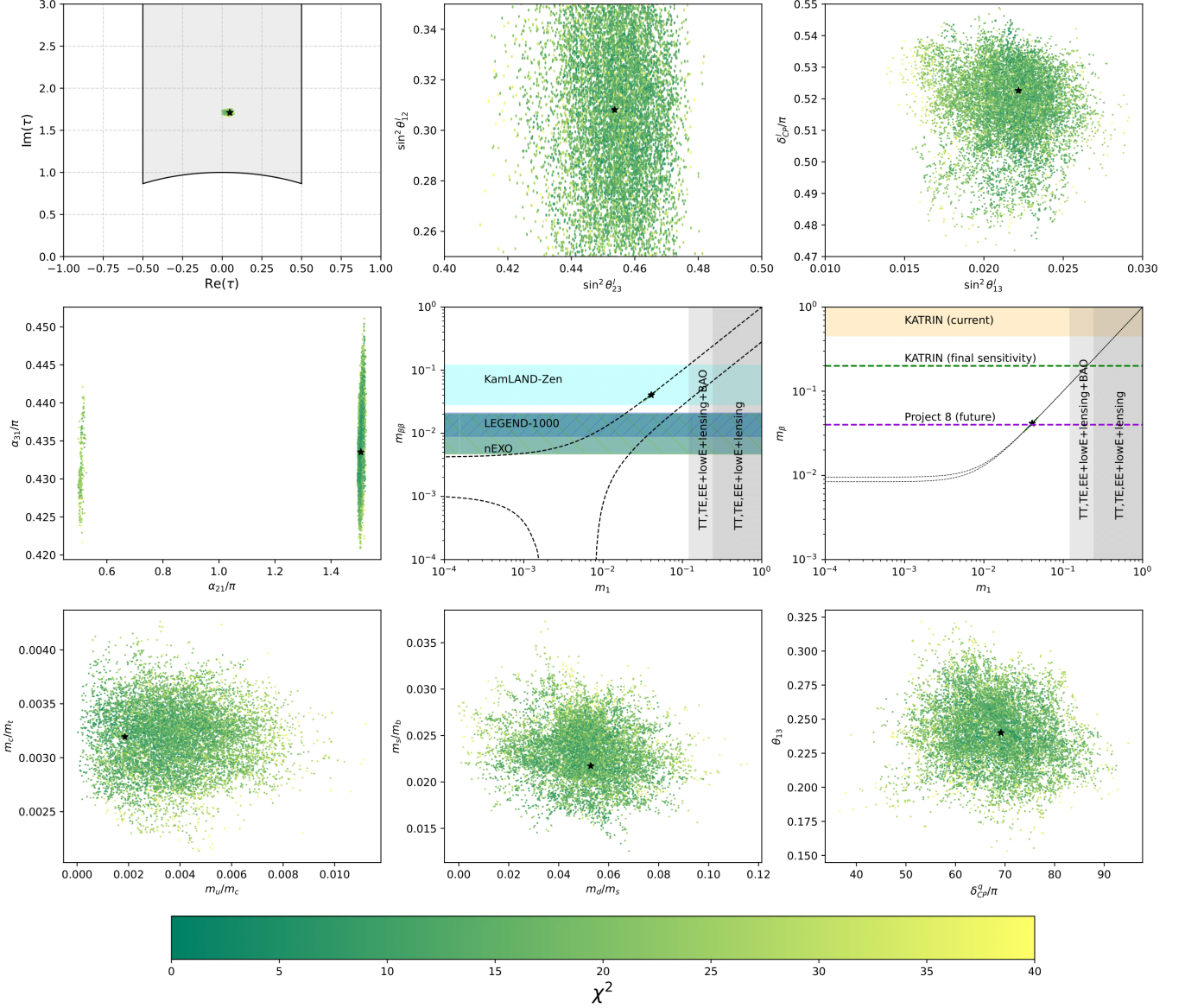


FIG. 2: Same as in figure 1 but for model II.

Beyond the benchmark models I and II discussed in the previous section, we investigated alternative configurations with different A_4 charge assignments for the matter fields. However, these models failed to yield viable solutions. For instance, when the 10-dimensional representation was assigned as an A_4 triplet and the three generations of the five-dimensional representation $\bar{5}_{F_i}$ were treated as A_4 singlets—while keeping the scalar sector trivial—no viable solutions emerged. Regardless of the weight assignments, which modify the resulting mass matrices, all cases resulted in χ^2_{total} values exceeding 50, with several observables falling outside their experimentally allowed 3σ range. The best-fit values of the free parameters for benchmark models I and II are summarized in Table IV for both neutrino mass hierarchies. The table also includes predictions for key observables, such as fermion mass ratios, flavor mixing parameters, the effective Majorana neutrino mass $m_{\beta\beta}$, the effective electron antineutrino mass m_β , as well as the three light neutrino masses $m_{i=1,2,3}$. Additionally, the table provides the minimum values of the χ^2 functions χ^2_l , χ^2_q and χ^2_{total} for both mass ordering. As shown in the last row of Table IV, the NO neutrino mass spectrum yields the lowest χ^2_{total} values for both models. In contrast, the IO spectrum results in a high $\chi^2_{total} > 10$ for model I but remains within 3σ agreement with data for model II with $\chi^2_{total} = 1.8303$. This suggests that model I favors only normal ordering, while model II allows both mass orderings.

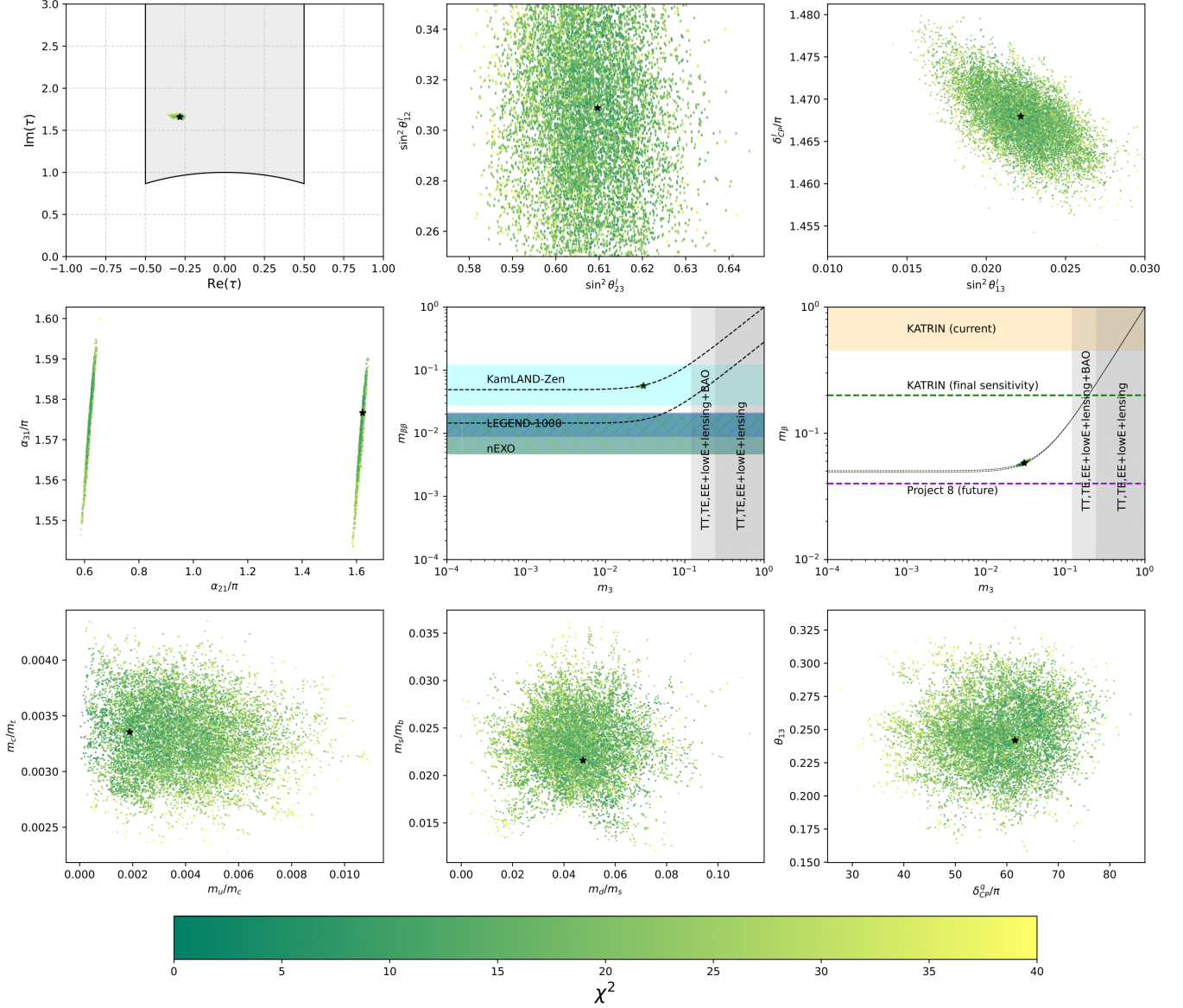


FIG. 3: Same as in figure 2 but for the inverted neutrino mass ordering.

Model I with a normal mass ordering is consistent with experimental data at the 3σ level, yielding a total chi-square value of $\chi_{\text{total}}^2 = 0.9106$. Among the 16 fitted observables, 12 fall within their 1σ experimentally allowed ranges, while the remaining four are within their 3σ limits. For model II with a normal mass ordering, we obtain $\chi_{\text{total}}^2 = 1.0136$, where 14 observables lie within their 1σ ranges. The observable $\sin^2 \theta_{23}^l$ is within its 3σ range, while δ_{CP}^l , the least constrained oscillation parameter, falls outside the 3σ bound. In the case of model II with an inverted mass ordering, the fit yields $\chi_{\text{total}}^2 = 1.8303$. Here, 13 observables are within their 1σ ranges, while two mass ratio observables (m_e/m_μ and m_c/m_t) are within their 3σ limits. However, $\sin^2 \theta_{23}^l$ lies outside the 3σ range. The correlations between the observables used in our numerical analysis are depicted in Figures 1, 2, and 3, corresponding to models I, II with NO, and model II with inverted ordering, respectively. In each figure, the first plot displays the allowed values of the modulus τ within the fundamental domain \mathcal{D} , represented by the gray region, with the best-fit value marked by a black star. For the NO case, τ is confined to a narrow region on the right side of \mathcal{D} in both models I and II (Figs. 1 and 2), whereas for the IO case in model II (3), it is located on the left side of \mathcal{D} . The second plot in the first row illustrates the correlation between $\sin^2 \theta_{12}^l$ and $\sin^2 \theta_{23}^l$. In model I (Figure 1), the atmospheric angle lies in the higher octant, with the best-fit value at $\sin^2 \theta_{23}^l = 0.510$. In model II with NO, $\sin^2 \theta_{23}^l$ is primarily in the lower octant, with a best-fit value of $\sin^2 \theta_{23}^l = 0.453$, whereas for the IO case, it lies in the higher octant but falls outside the 3σ range from NuFit 6.0. The best-fit value of the solar angle in all models remains consistent with the

NuFit 6.0 result: $\sin^2 \theta_{12}^l = 0.308$. The third figure in the first row presents the correlation between δ_{CP}^l and $\sin^2 \theta_{13}$. Model II predicts the leptonic Dirac CP phase most accurately in the IO case but falls outside the 3σ range in the NO case, whereas Model I remains within this 3σ range. The best-fit value of the reactor angle is consistently within 1σ level for all models.

The second row displays three plots showing the correlation between the two Majorana CP phases, α_{21} and α_{31} , and the effective neutrino masses, $m_{\beta\beta}$ and m_β , as functions of the lightest neutrino mass; m_1 for NO and m_3 for IO. The Majorana phases are well constrained in this study and deviate significantly from the CP-conserving values of 0 and π . In all models, the best-fit values are mostly around $\pi/2$. Specifically, in model I with NO, the phases are $\alpha_{21} \approx 1.544\pi$ and $\alpha_{31} \approx 1.574\pi$. In model II with NO, the values are $\alpha_{21} \approx 1.506\pi$ and $\alpha_{31} \approx 0.433\pi$. For model II with IO, the phases are $\alpha_{21} \approx 1.622\pi$ and $\alpha_{31} \approx 1.576\pi$. For the effective neutrino masses $m_{\beta\beta}$ and m_β , the plots for all models indicate that these parameters are tightly constrained, as the data points are closely clustered around their best-fit values. Below, we present the best-fit values for $m_{\beta\beta}$, m_β , the lightest neutrino mass, and the total sum of neutrino masses for each model

$$\begin{aligned} \text{Model I (NO):} \quad & m_{\beta\beta} = 131.28 \text{ meV}, \quad m_\beta = 76.53 \text{ meV}, \quad m_1 = 76.00 \text{ meV}, \quad \sum m_i = 243.52 \text{ meV} \\ \text{Model II (NO):} \quad & m_{\beta\beta} = 40.47 \text{ meV}, \quad m_\beta = 41.52 \text{ meV}, \quad m_1 = 40.55 \text{ meV}, \quad \sum m_i = 146.49 \text{ meV} \quad (\text{IV.26}) \\ \text{Model II (IO):} \quad & m_{\beta\beta} = 56.56 \text{ meV}, \quad m_\beta = 58.16 \text{ meV}, \quad m_3 = 30.09 \text{ meV}, \quad \sum m_i = 145.84 \text{ meV}. \end{aligned}$$

From the plots, it is evident that for all models, the predicted values of $m_{\beta\beta}$ fall within the region bounded by dashed lines, which correspond to the allowed range of $m_{\beta\beta}$ derived from the 3σ uncertainties in neutrino oscillation parameters. Moreover, these predictions remain consistent with the current most stringent constraint from the KamLAND-Zen collaboration represented by the cyan-shaded region. For m_β , the best-fit values across all models remain below both the current (orange shaded region) and future (green dashed line) projected sensitivities of the KATRIN experiment. If KATRIN fails to detect m_β within its future sensitivity limits, indicating that $m_\beta < 0.2$ eV, our predicted best-fit values could be tested by the upcoming Project 8 experiment, which aims to achieve a significantly improved sensitivity of approximately 0.04 eV [83]. In model I (NO), the best-fit value of the sum of neutrino masses in Eq. IV.27 is close to the upper limit set by the latest Planck cosmic microwave background constraints, which include the Planck power spectra and Planck lensing (TT , TE , EE + lowE + lensing), imposing an upper bound of $\sum m_i < 0.24$ eV. In model II, for both neutrino mass hierarchies, the sum of neutrino masses remains well below this upper bound, complying with the constraint. However, all models predict a best-fit value above the more stringent limit set by the Planck collaboration, which includes BAO, $\sum m_i < 0.12$ eV.

The last three panels of each figure focus on the quark sector, where the first two illustrate correlations among quark mass ratios, while the third presents the relationship between the Dirac CP phase and the third quark mixing angle. From the chi-square values associated with the quark sector (see the second-to-last row in Table IV), it is evident that all eight observables in our numerical analysis fall within the 3σ range. Notably, in the NO scenario, model II stands out with $\chi^2 \approx 0$, indicating that all observables lie within their 1σ allowed range.

V. UNIFICATION AND PROTON DECAY

A. Unification in $SU(5) \times \Gamma_3$ GUT

The SM does not achieve the exact GCU at a single energy scale. In fact, the running of gauge couplings shows that α_1 and α_2 unify around 10^{12-13} GeV, while α_2 and α_3 merge at a much higher scale, approximately 10^{16-17} GeV. This mismatch suggests the necessity of additional particles, as postulated in GUTs, to ensure precise unification. A viable solution is the introduction of scalar fields below the GUT scale M_X , which influence the evolution of gauge couplings through RGEs. Notably, scalars from the 45-dimensional Higgs representation in $SU(5)$ provide a well-motivated mechanism to achieve unification at experimentally viable energy scales [84–86]. In our construction, three Higgs fields— 5_H , 24_H , and 45_H —contribute to the RGEs of the gauge couplings. Their decomposition under SM

representations is given by

$$\begin{aligned}
5_H &= (3, 1, -\frac{1}{3}) \oplus (1, 2, \frac{1}{2}) \sim T \oplus H \\
24_H &= (8, 2, \frac{1}{2}) \oplus (1, 3, 0) \oplus (3, 2, -\frac{5}{6}) \oplus (\bar{3}, 2, \frac{5}{6}) \oplus \Sigma_1(1, 1, 0) \sim \Sigma_8 \oplus \Sigma_3 \oplus \Sigma_{(3,2)} \oplus \Sigma_{(\bar{3},2)} \oplus \Sigma_1 \\
45_H &= (\bar{3}, 1, \frac{4}{3}) \oplus (\bar{3}, 2, -\frac{7}{6}) \oplus (3, 3, -\frac{1}{3}) \oplus (6, 1, -\frac{1}{3}) \oplus (8, 2, \frac{1}{2}) \oplus (3, 1, -\frac{1}{3}) \oplus (1, 2, \frac{1}{2}) \\
&\sim \phi_1 \oplus \phi_2 \oplus \phi_3 \oplus \phi_4 \oplus \phi_5 \oplus T' \oplus H'
\end{aligned} \tag{V.27}$$

In our analysis, we assume that the SM gauge couplings are unified at the scale M_X , i.e., $\alpha_3(M_X) = \alpha_2(M_X) = \alpha_1(M_X) = \alpha_X(M_X)$, where we define $\alpha_3(\mu)$, $\alpha_2(\mu)$, and $\alpha_1(\mu)$ as

$$\alpha_3(\mu) = \alpha_s(\mu) = \frac{g_s(\mu)^2}{4\pi}, \quad \alpha_2(\mu) = \frac{g(\mu)^2}{4\pi}, \quad \alpha_1(\mu) = \frac{5}{3} \frac{g'(\mu)^2}{4\pi} \tag{V.28}$$

with g_s , g , and g' are the gauge coupling constants of $SU(3)_C$, $SU(2)_L$, and $U(1)_Y$, respectively. Under the unification assumption, the one-loop RGEs are solved, yielding the following solutions

$$\alpha_X^{-1}(M_X) = \alpha_3^{-1}(m_Z) - \left(\frac{B_{g_s}^{SM}}{2\pi} \log \frac{M_X}{m_Z} + \sum_{\chi} \frac{B_{g_s}^{\chi}}{2\pi} \log \frac{M_X}{m_{\chi}} \right), \tag{V.29}$$

$$\alpha_X^{-1}(M_X) = \alpha_2^{-1}(m_Z) - \left(\frac{B_g^{SM}}{2\pi} \log \frac{M_X}{m_Z} + \sum_{\chi} \frac{B_g^{\chi}}{2\pi} \log \frac{M_X}{m_{\chi}} \right), \tag{V.30}$$

$$\alpha_X^{-1}(M_X) = \alpha_1^{-1}(m_Z) - \frac{3}{5} \left(\frac{B_{g'}^{SM}}{2\pi} \log \frac{M_X}{m_Z} + \sum_{\chi} \frac{B_{g'}^{\chi}}{2\pi} \log \frac{M_X}{m_{\chi}} \right), \tag{V.31}$$

where m_Z is the mass of the Z -boson, χ runs over all relevant scalars, and the coefficients $B_{g_i}^{SM}$ and $B_{g_i}^{\chi}$ denote the beta functions of the three gauge couplings. They are given in Table (V). The relevant SM input parameters

| g_i | $B_{g_i}^{SM}$ | $B_{g_i}^{H'}$ | $B_{g_i}^T$ | $B_{g_i}^{T'}$ | $B_{g_i}^{\phi_1}$ | $B_{g_i}^{\phi_2}$ | $B_{g_i}^{\phi_3}$ | $B_{g_i}^{\phi_4}$ | $B_{g_i}^{\phi_5}$ | $B_{g_i}^{\Sigma_1}$ | $B_{g_i}^{\Sigma_3}$ | $B_{g_i}^{\Sigma_8}$ |
|-------|-----------------|----------------|---------------|----------------|--------------------|--------------------|--------------------|--------------------|--------------------|----------------------|----------------------|----------------------|
| g_s | -7 | 0 | $\frac{1}{6}$ | $\frac{1}{6}$ | $\frac{1}{6}$ | $\frac{1}{3}$ | $\frac{1}{2}$ | $\frac{5}{6}$ | 2 | 0 | 0 | $\frac{1}{2}$ |
| g | $-\frac{19}{6}$ | $\frac{1}{6}$ | 0 | 0 | 0 | $\frac{1}{2}$ | 2 | 0 | $\frac{4}{3}$ | 0 | $\frac{1}{3}$ | 0 |
| g' | $\frac{41}{6}$ | $\frac{1}{6}$ | $\frac{1}{9}$ | $\frac{1}{9}$ | $\frac{16}{9}$ | $\frac{49}{18}$ | $\frac{1}{3}$ | $\frac{2}{9}$ | $\frac{4}{3}$ | 0 | 0 | 0 |

TABLE V: Beta functions $B_{g_i}^{SM}$ and $B_{g_i}^{\chi}$ of the three gauge coupling constants

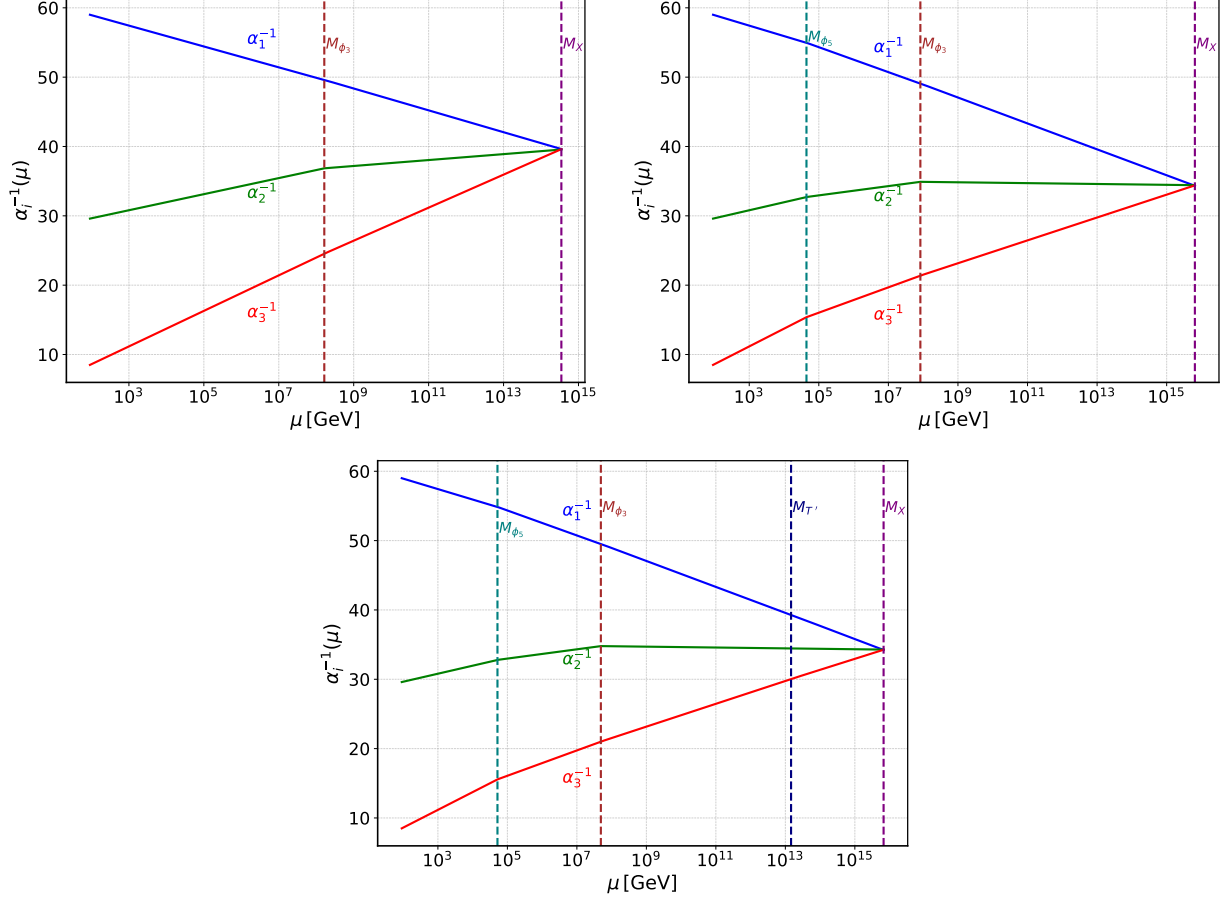
used in our analysis are the gauge boson mass $m_Z = 91.1876$ GeV, the gauge couplings $\alpha_s(m_Z) = 0.1193 \pm 0.0016$, $\alpha^{-1}(m_Z) = 127.906 \pm 0.019$, and the weak mixing angle $\sin^2 \theta_W(m_Z) = 0.23126 \pm 0.00005$ [3].

The mass splitting of the $SU(5)$ Higgs scalar 45_H components can impact the RG running of gauge couplings, potentially enhancing their unification. We examine scenarios where certain components remain significantly lighter than the unification scale M_X , making their contributions to the RG equations relevant at energy scales above their masses and altering the gauge coupling evolution. Specifically, we analyze cases that achieve GCU, considering configurations where one, two, or three scalar components lie below M_X and assessing their effects on gauge coupling unification.

Scenario I: One scalar component lighter than M_X

When a single scalar component remains lighter than M_X , GCU can occur at $M_X \sim \mathcal{O}(10^{14}$ GeV) [85]. In particular, the presence of the scalar triplet $\phi_3 \in H_{45}$ facilitates GCU when its mass is around $m_{\phi_3} \sim \mathcal{O}(10^8$ GeV). We explicitly demonstrate this scenario for specific scalar mass configurations in Table VI, while the resulting gauge coupling evolution is shown in the top left panel of Figure 4. This scenario, however, is subject to stringent constraints from proton decay experiments. Indeed, it is known that the unification scale M_X is tightly bounded due to contributions from the exchange of the heavy $SU(5)$ gauge bosons X and Y , leading to baryon-number-violating dimension-six operators, which induce too fast proton decay [87]. Current experimental bounds on the proton lifetime $\tau_p(p \rightarrow e^+ \pi^0) > 2.4 \times 10^{34}$ yrs, impose a lower bound of $M_X > 5 \times 10^{15}$ GeV [15]. Consequently, this scenario is excluded by the current proton decay constraints.

| M_X | $M_{H'}, M_T, M_{T'}$ | M_{ϕ_3} | $M_{\phi_1}, M_{\phi_2}, M_{\phi_4}, M_{\phi_5}$ |
|-----------------------|-----------------------|--------------------|--|
| 3.49×10^{14} | 3.49×10^{14} | 1.64×10^8 | 3.49×10^{14} |
| 3.70×10^{14} | 3.70×10^{14} | 1.62×10^8 | 3.70×10^{14} |

TABLE VI: Mass spectrum of scalar components for successful grand unification at $M_X \sim \mathcal{O}(10^{14} \text{ GeV})$ FIG. 4: Renormalization group evolution of gauge coupling constants for three scenarios. Top left panel: Single light scalar ϕ_3 below M_X . Top right panel: Two light scalar components, ϕ_3 and ϕ_5 , contributing to the running. Bottom panel: Three light scalar components, ϕ_3 , ϕ_5 and T' , affecting the gauge coupling unification.**Scenario II: Two scalar components lighter than M_X**

To address the issue of rapid proton decay mediated by the exchange of X and Y gauge bosons, the unification scale M_X must be significantly increased. In this scenario we consider two scalar components, ϕ_3 and ϕ_5 , with masses below M_X , providing a viable framework for achieving GCU at a scale of $\mathcal{O}(10^{15} \text{ GeV})$. We find that the typical mass values are $M_{\phi_3} \sim \mathcal{O}(10^7 \text{ GeV})$ for the scalar color triplet, and $M_{\phi_5} \sim \mathcal{O}(10^4 \text{ GeV})$ for the scalar color octet. The mass spectra for three representative examples are summarized in Table VII. The mass hierarchy of the scalar

| M_X | $M_{H'}, M_{T'}, M_T$ | $M_{\phi_1}, M_{\phi_2}, M_{\phi_4}$ | M_{ϕ_3} | M_{ϕ_5} | $M_{\Sigma_8}, M_{\Sigma_3}$ |
|-----------------------|-----------------------|--------------------------------------|--------------------|--------------------|------------------------------|
| 6.47×10^{15} | 6.47×10^{15} | 6.47×10^{15} | 8.31×10^7 | 4.42×10^4 | 6.47×10^{15} |
| 7.34×10^{15} | 7.34×10^{15} | 7.34×10^{15} | 7.03×10^7 | 1.42×10^4 | 7.34×10^{15} |
| 7.89×10^{15} | 7.89×10^{15} | 7.89×10^{15} | 7.06×10^7 | 9.13×10^3 | 7.89×10^{15} |

TABLE VII: Mass spectrum of scalar components for successful GCU at $M_X \sim \mathcal{O}(10^{15} \text{ GeV})$.

components, as shown in Table VII, demonstrate that the GCU is successfully achieved with the GUT scale raised to approximately $M_X \sim 7 \times 10^{15}$ GeV. This increase in M_X ensures compatibility with experimental constraints on proton lifetime, as the contributions to proton decay from X and Y gauge bosons exchange are sufficiently suppressed. The impact of the selected mass spectra on the evolution of the gauge couplings is illustrated in the top right panel of Figure 4, which displays the unification of the couplings at the predicted scale.

Scenario III: Three scalar components bellow M_X

A scenario with three light scalar components below M_X provides an alternative route to achieving GCU. In this case, the light components can be identified as T' , ϕ_3 , and ϕ_5 from the 45_H multiplet. Compared to scenario II, this setup offers additional possibilities for unification while ensuring compatibility with the experimental constraint $M_X > 5 \times 10^{15}$ GeV, which is necessary to suppress rapid proton decay. We present specific examples of scalar

| M_X | $M_{H'}, M_T$ | $M_{T'}$ | $M_{\phi_1}, M_{\phi_2}, M_{\phi_4}$ | M_{ϕ_3} | M_{ϕ_5} | $M_{\Sigma_8}, M_{\Sigma_3}$ |
|-----------------------|-----------------------|-----------------------|--------------------------------------|--------------------|--------------------|------------------------------|
| 6.72×10^{15} | 6.72×10^{15} | 1.51×10^{13} | 6.72×10^{15} | 4.84×10^7 | 5.46×10^4 | 6.72×10^{15} |
| 7.31×10^{15} | 7.31×10^{15} | 1.33×10^{13} | 7.31×10^{15} | 5.17×10^7 | 3.78×10^4 | 7.31×10^{15} |

TABLE VIII: Mass spectrum of scalar components for successful Grand Unification at $M_X \sim \mathcal{O}(10^{15})$ GeV).

mass spectra that achieve GCU in Table (VIII). The resulting mass hierarchy for the three scalars ensures that the unification scale remains around $M_X \sim 7 \times 10^{15}$ GeV. This, in turn, suppresses contributions from the X and Y gauge bosons. The evolution of the gauge couplings for these configurations is shown in the bottom panel of Figure 4, where successful unification at the GUT scale is evident.

B. Proton decay

In $SU(5)$ GUT with 45_H Higgs, five scalar multiplets contribute to proton decay; the gauge bosons X, Y , the $SU(3)$ triplets $T \sim (3, 1, -\frac{1}{3}) \subset 5_H$, $T' \sim (3, 3, -\frac{1}{3})$, $\phi_3 \sim (3, 3, -\frac{1}{3})$, and $\phi_1 \sim (\bar{3}, 1, \frac{4}{3}) \subset 45_H$. These multiplets contribute to dimension-six operators responsible for Higgs-mediated proton decay. The three scenarios discussed above emphasize the critical role of a light scalar ϕ_3 in achieving GCU at sufficiently high energy scale M_X . This is driven by the necessity to suppress the gauge-mediated proton decay processes. However, the mass of ϕ_3 cannot be arbitrarily light, as it mediates fast proton decay through operators arising from the Yukawa interactions $Y_{45}^{ij} 10_{F_i} 5_{F_j} 45_H^*$ and $Y_{45}^{ij} 10_{F_i} 10_{F_j} 45_H$. Consequently, the mass of ϕ_3 must be constrained to satisfy experimental limits on the proton lifetime. For a detailed review on this topic, see Refs. [87, 88]. To prevent rapid proton decay mediated by Higgs triplets, their masses must exceed approximately 3×10^{10} GeV, assuming natural values for the Yukawa couplings [89]. However, if any of these fields is significantly lighter than the GUT scale, their Yukawa couplings must be sufficiently suppressed to remain consistent with experimental constraints on the proton lifetime.

To address the tension between GUT constraints and proton decay limits in our framework, we propose a scenario in which the masses of the X and Y gauge bosons, along with T, T' and ϕ_1 scalar triplets, are set at the scale $\mathcal{O}(10^{15})$ GeV. However, considering all scalar triplets at the GUT scale generally prevents the successful realization of GCU. Therefore, we impose a mass hierarchy where ϕ_3 is fixed slightly below the GUT scale, playing the most important role in ensuring GCU. The remaining components of the 45_H Higgs field, specifically ϕ_2, ϕ_4 , and ϕ_5 , along with the components of the 24_H , namely Σ_3 and Σ_8 , do not directly participate in proton decay processes. This allows for greater flexibility in assigning their masses while maintaining consistency with unification constraints. In this context, we achieve the unification of gauge couplings with the mass spectrum $M_X = M_{\phi_2} = M_{\phi_4} = M_{\Sigma_3} = M_{\Sigma_8} = 7.916 \times 10^{15}$ GeV, ensuring that these fields remain at the GUT scale without disrupting the GCU. On the other hand, the color octet ϕ_5 , which does not mediate proton decay, is set at $M_{\phi_5} = 8.757 \times 10^3$ GeV to comply with collider constraints. These constraints require that $M_{\phi_5} > 3.1$ TeV for natural Yukawa couplings [90]. Meanwhile, the mass of ϕ_3 is set to $M_{\phi_3} = 6.076 \times 10^7$ GeV, which plays a crucial role in achieving GCU. The impact of ϕ_3 on proton decay constraints will be analyzed below. We show in Figure 5 the RG evolution of the gauge couplings for this mass spectrum, illustrating their successful convergence at the unification scale.

Consider the proton lifetime in the decay process $p \rightarrow e^+ \pi^0$, which is mediated by the scalar field ϕ_3 with a mass of $M_{\phi_3} = 6.076 \times 10^7$ GeV. The associated dimension-6 operator, responsible for this decay, arises from the following interactions:

$$(Y_{45})_{ij} Q^T L \phi_3^*, \quad (Y_{45})_{ij} Q^T Q \phi_3. \quad (\text{V.32})$$

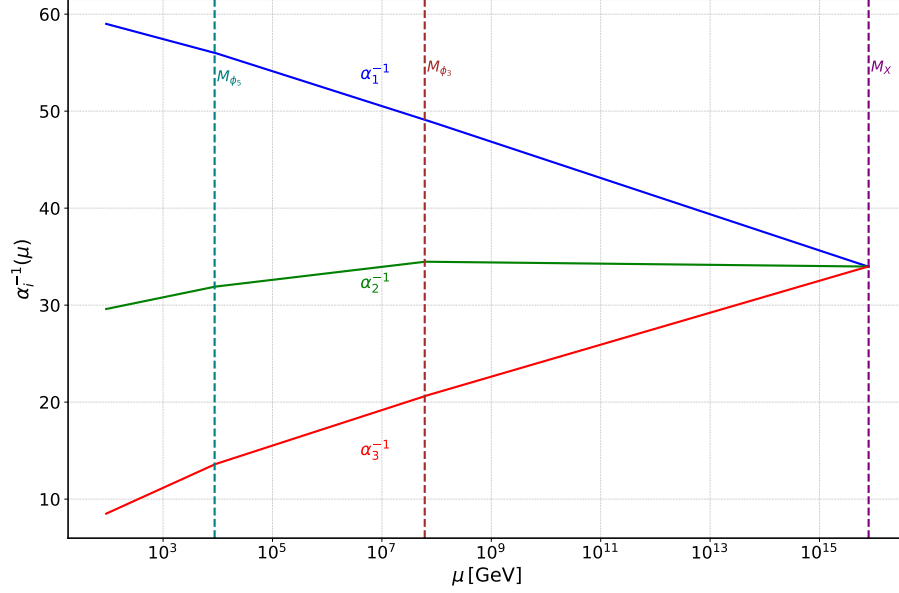


FIG. 5: Evolution of gauge coupling constants in scenario where the scalar triplet ϕ_3 and the octet ϕ_5 , are set below the unification scale M_X .

Consequently, the lifetime is estimated as

$$\tau_p \sim \frac{M_{\phi_3}^4}{|(Y_{45})_{11}(Y_{45})_{11}|^2 m_p^5}, \quad (\text{V.33})$$

where $m_p \approx 0.94$ GeV is the proton mass. In the context of model I with NO, the Yukawa coupling $(Y_{45})_{11}$ is expressed as $(Y_{45})_{11} = b'_1 Y_{3,2}^{(2)}$. Using the parameter values $|Y_{3,2}^{(2)}| = 0.1769$, $(b'_1/b_3) = 0.5024$, and $b_3 v = 57.8613$ GeV from Table (IV), we obtain $|(Y_{45})_{11}| = 2.0904 \times 10^{-2}$. Substituting this value into the relation V.33 and imposing the current experimental bound $\tau_p(p \rightarrow e^+ \pi^0) > 2.4 \times 10^{34}$ years[15], we find that ensuring the stability of the proton requires $|(Y_{45})_{11}| \lesssim 1.92 \times 10^{-16}$. This stringent upper bound indicates that the contribution of the Yukawa term $Y_{45} 10_{F_i} 10_{F_i} 45_H$ to the up-quark mass matrix is negligibly small, thereby reinforcing the suppression of proton decay. Applying this constraint for the other models using the best-fit values of the parameters in Table IV, we obtain as well highly suppressed Yukawa couplings where the upper limits are as follows for $|(Y_{45})_{11}|$:

$$\begin{aligned} \text{Model II (NO): } & |(Y_{45})_{11}| \lesssim 2.17 \times 10^{-15}, \\ \text{Model II (IO): } & |(Y_{45})_{11}| \lesssim 3.95 \times 10^{-15}. \end{aligned} \quad (\text{V.34})$$

The omission of the coupling $Y_{45} 10_{F_i} \cdot 10_{F_i} \cdot 45_H$ in our benchmark models is well justified, as its impact on the up-quark mass matrix remains too small to have any significant phenomenological consequences. Beyond the specific assumptions imposed in our benchmark models, additional theoretical mechanisms may be necessary to ensure a more fundamental suppression of this coupling. A particular way in the context of A_4 modular invariance, is to assign modular weights for the 45_H such that polyharmonic Maaß forms $Y_r^{k_Y}$ that could generate the operator $Y_r^{k_Y} 10_{F_i} \cdot 10_{F_i} \cdot 45_H$ are forbidden. This can be enforced by the modular weight constraint $k_Y \neq k_{10_i} + k_{10_j} + k_{45_H}$, which ensures that no modular form contributes to this interaction, thereby eliminating its effects on the up-quark sector. As a result, proton decay mediated by the triplet scalar component ϕ_3 , through the interactions $Y_{45} 10_{F_i} \cdot 10_{F_i} \cdot 45_H$ and $Y_{45} 10_{F_i} \cdot 5_{F_i} \cdot 45_H^*$ is completely absent.

VI. SUMMARY AND CONCLUSIONS

This work introduces non-holomorphic A_4 modular symmetry into $SU(5)$ GUT for the first time, providing a unified framework that addresses flavor puzzle and ensures gauge coupling unification. Specifically, we have employed polyharmonic Maaß forms of level $N = 3$ and developed two benchmark models which differ from each other by modular weight and A_4 charge assignments. After providing the corresponding fermion Yukawa matrices, a numerical

scan over the parameter space of each model, including the real and imaginary parts of the modulus τ , was performed to minimize the total chi-square function χ^2_{total} and optimize agreement with experimental data. Our analysis demonstrates excellent consistency with experimental results across both the lepton and quark sectors, achieving $\chi^2_{\text{total}} < 10$, as shown in Table IV. The results indicate that model I favors only the NO mass spectrum, while model II accommodates both mass orderings.

For neutrino observables, all models yield predictions consistent with the 3σ ranges from NuFit 6.0, with the exception of a single observable in Model II. Specifically, in the NO scenario, the CP -violating phase δ_{CP}^l lies outside the 3σ range, while in the IO case, $\sin^2 \theta_{23}$ exceeds its allowed bounds. The atmospheric mixing angle θ_{23}^l is predicted to be in the higher octant for NO in model I and IO in model II, while it lies in the lower octant for NO in model II. Additionally, the two Majorana CP phases, α_{21} and α_{31} , significantly deviate from the CP -conserving values of 0 and π , with best-fit values clustering around $\pi/2$. For predictions on the absolute neutrino mass scale, the mass parameters $m_{\beta\beta}$, $\sum m_i$, and m_β align with current experimental constraints and provide insights into upcoming detection capabilities. Regarding $m_{\beta\beta}$, the predicted values for all models are consistent with the current most stringent constraint from the KamLAND-Zen collaboration. Similarly, for m_β , all models yield best-fit values that remain below both current and future sensitivities of the KATRIN experiment. Meanwhile, the predicted values could be tested by the upcoming Project 8 experiment. The sum of neutrino masses, $\sum m_i$, for the three models satisfies the limit provided by the latest Planck CMB measurements (TT, TE, EE + lowE + lensing) $\sum m_i < 0.24$ eV and falls within the sensitivity range of future experiments. For the charged lepton mass ratios, they are in agreement with their 1σ level for both models in the NO case, while for model II with IO, they are within their 3σ range. For the quark observables, we found that they align with data at the GUT scale within 3σ level. Notably, in the case of model II with NO, all the observables are within the 1σ level with $\chi^2 \approx 0$.

The 45_H Higgs field plays a crucial role in resolving the mass hierarchy between charged leptons and down-type quarks while significantly influencing the RG evolution of gauge couplings. Accordingly, GCU is achieved at $M_X \approx 7.9 \times 10^{15}$ GeV due to threshold corrections from light scalar components of 45_H . Notably, a color-triplet scalar ϕ_3 with $M_{\phi_3} \approx 6 \times 10^7$ GeV and a color-octet scalar ϕ_5 with $M_{\phi_5} \approx 8.7 \times 10^3$ GeV—consistent with the collider constraint $M_{\phi_5} > 3.1$ TeV—play key roles in achieving unification. Proton decay via the scalar triplets $T \in 5_H$ and $T', \phi_1 \in 45_H$ is suppressed due to their GUT-scale masses, while decay via $\phi_3 \in 45_H$ is further suppressed by stringent Yukawa constraints, $|Y_{45})_{11}| \lesssim 10^{-15}$, ensuring compatibility with experimental bounds on $p \rightarrow e^+ \pi^0$ lifetimes.

This study highlights the viability of non-holomorphic modular flavor symmetries as a bridge between GUT frameworks and observed flavor structures, offering a minimalist alternative to supersymmetric approaches. Future investigations may extend this approach by exploring other modular groups, such as S_4 and A_5 or incorporating additional Higgs representations to further refine mass predictions. The viability of this framework will be tested through experimental probes of neutrino mass ordering and leptonic CP violation.

Acknowledgements

The work of M.A.L. and S.N. is supported by the United Arab Emirates University (UAEU) under UPAR Grant No. 12S093.

Appendix A: Finite modular group of level 3

The finite modular group Γ_3 is isomorphic to the non-Abelian group A_4 , which represents the symmetry group of a tetrahedron and consists of the even permutations of four objects. This group is generated by two elements, S and T , satisfying the relations $S^2 = (ST)^3 = T^3 = 1$. The order of A_4 is given by $4!/2 = 12$, and its elements are distributed among four conjugacy classes

$$C_1 = \{e\}, \quad C_3 = \{S, TST^2, T^2ST\}, \quad C_4 = \{T, ST, TS, STS\}, \quad C_{4'} = \{T^2, ST^2, T^2S, ST^2S\}. \quad (\text{A.1})$$

Since the A_4 group has four conjugacy classes, it must also have four irreducible representations. These consist of three one-dimensional representations⁶, $\mathbf{1}$, $\mathbf{1}'$, $\mathbf{1}''$, and a single three-dimensional representation, $\mathbf{3}$. The representation

⁶ The three one-dimensional representations can be distinguished by their basis characters as $\mathbf{1}_{(1,1)}$, $\mathbf{1}_{(1,\omega)}$, $\mathbf{1}_{(1,\omega^2)}$, where the entries (x, y) denote the characters of the S and T generators, respectively. For further details on this character notation, see Refs. [91, 92].

matrices for the A_4 generators in the T-diagonal basis are of the following form for the four different representations

$$\begin{aligned}
\mathbf{1} &: S = 1, \quad T = 1 \\
\mathbf{1}' &: S = 1, \quad T = \omega \\
\mathbf{1}'' &: S = 1, \quad T = \omega^2 \\
\mathbf{3} &: S = \begin{pmatrix} -1 & 2 & 2 \\ 2 & -1 & 2 \\ 2 & 2 & -1 \end{pmatrix}, \quad T = \begin{pmatrix} 1 & 0 & 0 \\ 0 & \omega & 0 \\ 0 & 0 & \omega^2 \end{pmatrix}.
\end{aligned} \tag{A.2}$$

with ω being the cube root of unity: $\omega = e^{2\pi i/3}$. The tensor product rules for the irreducible representations of the A_4 group

$$\mathbf{1} \otimes \mathbf{r} = \mathbf{r}, \quad \mathbf{1}' \otimes \mathbf{1}' = \mathbf{1}'', \quad \mathbf{1}' \otimes \mathbf{1}'' = \mathbf{1}, \quad \mathbf{1}'' \otimes \mathbf{1}'' = \mathbf{1}', \quad \mathbf{3} \otimes \mathbf{3} = \mathbf{1} \oplus \mathbf{1}' \oplus \mathbf{1}'' \oplus \mathbf{3}_S \oplus \mathbf{3}_A, \tag{A.3}$$

where \mathbf{r} denotes any irreducible representation of A_4 , while $\mathbf{3}_S$ and $\mathbf{3}_A$ stands for the symmetric and the antisymmetric contractions, respectively. The contraction rules for two generic A_4 triplets, $a = (a_1, a_2, a_3)^T$ and $b = (b_1, b_2, b_3)^T$, follow from the given tensor product decomposition where we have

$$\begin{aligned}
(a \otimes b)|_{\mathbf{1}} &= a_1 b_1 + a_2 b_3 + a_3 b_2 \\
(a \otimes b)|_{\mathbf{1}'} &= a_3 b_3 + a_1 b_2 + a_2 b_1 \\
(a \otimes b)|_{\mathbf{1}''} &= a_2 b_2 + a_1 b_3 + a_3 b_1 \\
(a \otimes b)|_{\mathbf{3}_S} &= (2a_1 b_1 - a_2 b_3 - a_3 b_2, 2a_3 b_3 - a_1 b_2 - a_2 b_1, 2a_2 b_2 - a_1 b_3 - a_3 b_1)^T \\
(a \otimes b)|_{\mathbf{3}_A} &= (a_2 b_3 - a_3 b_2, a_1 b_2 - a_2 b_1, a_3 b_1 - a_1 b_3)^T
\end{aligned} \tag{A.4}$$

We now present the explicit expressions for the polyharmonic Maaß forms $Y_{\mathbf{r}}^{(k_Y)}$ used in our benchmark models, as listed in Tables I and II. Notice that these forms correspond to the known modular forms of level N and weight $k \geq 4$, since modular forms with negative weight do not exist [32]. Moreover, as previously noted, their weight for Γ_N is an even integer, where in our case, with $N = 3$, the corresponding finite modular group is the alternating group A_4 . For our benchmark model I, we have employed polyharmonic Maaß forms with weights $k_Y = -2, 0, 2, 4, 6$.

- $k_Y = -2$: the weight $k_Y = -2$ polyharmonic Maaß forms can be organized into a trivial singlet $Y_1^{(-2)}(\tau)$ and a triplet $Y_3^{(-2)}(\tau) = [Y_{3,1}^{(-2)}(\tau), Y_{3,2}^{(-2)}(\tau), Y_{3,3}^{(-2)}(\tau)]$ of A_4 . Their Fourier expansion is given by [32]

$$\begin{aligned}
Y_1^{(-2)}(\tau) &= \frac{y^3}{3} - \frac{15\Gamma(3, 4\pi y)}{4\pi^3 q} - \frac{135\Gamma(3, 8\pi y)}{32\pi^3 q^2} - \frac{35\Gamma(3, 12\pi y)}{9\pi^3 q^3} + \dots \\
&\quad - \frac{\pi}{12} \frac{\zeta(3)}{\zeta(4)} - \frac{15q}{2\pi^3} - \frac{135q^2}{16\pi^3} - \frac{70q^3}{9\pi^3} - \frac{1095q^4}{128\pi^3} - \frac{189q^5}{25\pi^3} + \dots
\end{aligned} \tag{A.5}$$

$$\begin{aligned}
Y_{3,1}^{(-2)}(\tau) &= \frac{y^3}{3} + \frac{21\Gamma(3, 4\pi y)}{16\pi^3 q} + \frac{189\Gamma(3, 8\pi y)}{128\pi^3 q^2} + \frac{169\Gamma(3, 12\pi y)}{144\pi^3 q^3} + \dots \\
&\quad + \frac{\pi}{40} \frac{\zeta(3)}{\zeta(4)} + \frac{21q}{8\pi^3} + \frac{189q^2}{64\pi^3} + \frac{169q^3}{72\pi^3} + \frac{1533q^4}{512\pi^3} + \frac{1323q^5}{500\pi^3} + \dots
\end{aligned} \tag{A.6}$$

$$\begin{aligned}
Y_{3,2}^{(-2)}(\tau) &= -\frac{729q^{1/3}}{16\pi^3} \left(\frac{\Gamma(3, 8\pi y/3)}{16q} + \frac{7\Gamma(3, 20\pi y/3)}{125q^2} + \frac{65\Gamma(3, 32\pi y/3)}{1024q^3} + \dots \right) \\
&\quad - \frac{81q^{1/3}}{16\pi^3} \left(1 + \frac{73q}{64} + \frac{344q^2}{343} + \frac{567q^3}{500} + \frac{20198q^4}{2197} + \frac{4681q^5}{4096} + \dots \right)
\end{aligned} \tag{A.7}$$

$$\begin{aligned}
Y_{3,3}^{(-2)}(\tau) &= -\frac{81q^{2/3}}{32\pi^3} \left(\frac{\Gamma(3, 4\pi y/3)}{q} + \frac{73\Gamma(3, 16\pi y/3)}{64q^2} + \frac{344\Gamma(3, 28\pi y/3)}{343q^3} + \dots \right) \\
&\quad - \frac{729q^{2/3}}{8\pi^3} \left(\frac{1}{16} + \frac{7q}{125} + \frac{65q^2}{1024} + \frac{74q^3}{1331} + \dots \right)
\end{aligned} \tag{A.8}$$

- $k_Y = 0$: the weight $k_Y = 0$ polyharmonic Maaß forms can be organized into a trivial singlet $Y_1^{(0)}(\tau) = 1$ and an A_4 triplet $Y_3^{(0)}(\tau) = [Y_{3,1}^{(0)}(\tau), Y_{3,2}^{(0)}(\tau), Y_{3,3}^{(0)}(\tau)]$ where their q-expansion are given by

$$Y_{3,1}^{(0)} = y - 3\frac{e^{-4\pi y}}{\pi q} - 9\frac{e^{-8\pi y}}{2\pi q^2} - \frac{e^{-12\pi y}}{\pi q^3} - 21\frac{e^{-16\pi y}}{4\pi q^4} - 18\frac{e^{-20\pi y}}{5\pi q^5} + \dots$$

$$- \frac{9 \log 3}{4\pi} - \frac{3q}{\pi} - \frac{9q^2}{2\pi} - \frac{q^3}{\pi} - \frac{21q^4}{4\pi} - \frac{18q^5}{5\pi} - \frac{3q^6}{2\pi} + \dots \quad (\text{A.9})$$

$$Y_{3,2}^{(0)} = \frac{27q^{1/3}e^{\pi y/3}}{\pi} \left(\frac{e^{-3\pi y}}{4q} + \frac{e^{-7\pi y}}{5q^2} + \frac{5e^{-11\pi y}}{16q^3} + \frac{2e^{-15\pi y}}{11q^4} + \frac{2e^{-19\pi y}}{7q^5} + \dots \right)$$

$$+ \frac{9q^{1/3}}{2\pi} \left(1 + \frac{7q}{4} + \frac{8q^2}{7} + \frac{9q^3}{5} + \frac{14q^4}{13} + \frac{31q^5}{16} + \frac{20q^6}{19} + \dots \right) \quad (\text{A.10})$$

$$Y_{3,3}^{(0)} = \frac{9q^{2/3}e^{2\pi y/3}}{2\pi} \left(\frac{e^{-2\pi y}}{q} + \frac{7e^{-6\pi y}}{4q^2} + \frac{8e^{-10\pi y}}{7q^3} + \frac{9e^{-14\pi y}}{5q^4} + \frac{14e^{-18\pi y}}{13q^5} + \dots \right)$$

$$+ \frac{27q^{2/3}}{\pi} \left(\frac{1}{4} + \frac{q}{5} + \frac{5q^2}{16} + \frac{2q^3}{11} + \frac{2q^4}{7} + \frac{9q^5}{17} + \frac{21q^6}{20} + \dots \right) \quad (\text{A.11})$$

- $k_Y = 2$: The weight 2 polyharmonic Maaß forms consist of the modified Eisenstein series $\hat{E}_2(\tau)$, which is a trivial singlet under A_4 , and the modular form triplets of weight 2 and level 3, denoted as $Y_3^{(2)}(\tau) = (Y_1(\tau), Y_2(\tau), Y_3(\tau))^T$. The modified Eisenstein series is defined as

$$\hat{E}_2(\tau) = E_2(\tau) - \frac{3}{\pi y} \quad (\text{A.12})$$

where $E_2(\tau)$ is the weight 2 Eisenstein series expressed as $E_2(\tau) = 1 - 24 \sum_{n=1}^{\infty} \sigma_1(n)q^n$ with $\sigma_1(n) = \sum_{d|n} d$ is the sum of the divisors of n . The q-expansions of the components of the triplet $Y_3^{(2)}(\tau)$ are given as follows [22]

$$Y_1(\tau) = 1 + 12q + 36q^2 + \dots, \quad Y_2(\tau) = -6q^{1/3}(1 + 7q + 8q^2 + \dots), \quad Y_3(\tau) = -18q^{2/3}(1 + 2q + 5q^2 + \dots). \quad (\text{A.13})$$

- $k_Y = 4$: Weight 4 polyharmonic Maaß forms correspond to modular forms at level 3. These forms arise from the tensor product $Y_3^{(2)}(\tau) \otimes Y_3^{(2)}(\tau)$, which decomposes into a trivial singlet $Y_1^{(4)}(\tau)$, a nontrivial singlet $Y_{1'}^{(4)}(\tau)$, and an A_4 triplet $Y_3^{(4)}(\tau)$, whose explicit expressions are given as follows

$$Y_1^{(4)}(\tau) = Y_1^2(\tau) + 2Y_2(\tau)Y_3(\tau)$$

$$Y_{1'}^{(4)}(\tau) = Y_3^2(\tau) + 2Y_1(\tau)Y_2(\tau) \quad (\text{A.14})$$

$$Y_3^{(4)}(\tau) = (Y_1^2(\tau) - Y_2(\tau)Y_3(\tau), Y_3^2(\tau) - Y_1(\tau)Y_2(\tau), Y_2^2(\tau) + 2Y_1(\tau)Y_3(\tau))^T.$$

- $k_Y = 6$: Similar to the preceding case, weight 6 polyharmonic Maaß forms correspond to modular forms at level 3. There are three such forms: a trivial singlet $Y_1^{(6)}(\tau)$ and two A_4 triplets denoted as $Y_{3I}^{(6)}(\tau)$ and $Y_{3II}^{(6)}(\tau)$ [32]. In our benchmark model I, we used only the trivial singlet which is expressed as: $Y_1^{(6)}(\tau) = Y_1^3(\tau) + Y_2^3(\tau) + Y_3^3(\tau) - 3Y_1(\tau)Y_2(\tau)Y_3(\tau)$.

In our benchmark model II, we have employed polyharmonic Maaß forms with weights $k_Y = -4, -2, 4, 6$. The explicit expressions of the weights $-2, 4$ and 6 polyharmonic Maaß forms are given in the previous case of model I, while weight -4 polyharmonic Maaß forms consist of a trivial singlet $Y_1^{(-4)}(\tau)$ and an A_4 triplet $Y_3^{(-4)}(\tau) = [Y_{3,1}^{(-4)}(\tau), Y_{3,2}^{(-4)}(\tau), Y_{3,3}^{(-4)}(\tau)]$ expressed as [32]

$$Y_1^{(-4)} = \frac{y^5}{5} + \frac{63\Gamma(5, 4\pi y)}{128\pi^5 q} + \frac{2079\Gamma(5, 8\pi y)}{4096\pi^5 q^2} + \frac{427\Gamma(5, 12\pi y)}{864\pi^5 q^3} + \dots$$

$$+ \frac{\pi}{80} \frac{\zeta(5)}{\zeta(6)} + \frac{189q}{16\pi^5} + \frac{6237q^2}{512\pi^5} + \dots \quad (\text{A.15})$$

$$Y_{3,1}^{(-4)} = \frac{y^5}{5} - \frac{549}{3328\pi^5} \left(\frac{\Gamma(5, 4\pi y)}{q} + \frac{33\Gamma(5, 8\pi y)}{32q^2} + \frac{14641\Gamma(5, 12\pi y)}{14823q^3} + \dots \right) - \frac{3\pi}{728} \frac{\zeta(5)}{\zeta(6)} - \frac{1647}{416\pi^5} \left(q + \frac{33q^2}{32} + \frac{14641q^3}{14823} + \dots \right) \quad (\text{A.16})$$

$$Y_{3,2}^{(-4)} = \frac{72171q^{1/3}}{212992\pi^5} \left(\frac{\Gamma(5, 8\pi y/3)}{q} + \frac{33344\Gamma(5, 20\pi y/3)}{34375q^2} + \frac{1025\Gamma(5, 32\pi y/3)}{1024q^3} + \dots \right) + \frac{6561q^{1/3}}{832\pi^5} \left(1 + \frac{1057q}{1024} + \frac{16808q^2}{16807} + \dots \right) \quad (\text{A.17})$$

$$Y_{3,3}^{(-4)} = \frac{2187q^{2/3}}{6656\pi^5} \left(\frac{\Gamma(5, 4\pi y/3)}{q} + \frac{1057\Gamma(5, 16\pi y/3)}{1024q^2} + \frac{16808\Gamma(5, 28\pi y/3)}{16807q^3} + \dots \right) + \frac{216513q^{2/3}}{26624\pi^5} \left(1 + \frac{33344q}{34375} + \frac{1025q^2}{1024} + \frac{1717888q^3}{1771561} + \frac{16808q^4}{16807} + \dots \right) \quad (\text{A.18})$$

-
- [1] **Super-Kamiokande** Collaboration, Y. Fukuda et al., *Evidence for oscillation of atmospheric neutrinos*, *Phys. Rev. Lett.* **81** (1998) 1562–1567, [[hep-ex/9807003](#)].
- [2] **SNO** Collaboration, Q. R. Ahmad et al., *Direct evidence for neutrino flavor transformation from neutral current interactions in the Sudbury Neutrino Observatory*, *Phys. Rev. Lett.* **89** (2002) 011301, [[nucl-ex/0204008](#)].
- [3] **Particle Data Group** Collaboration, S. Navas et al., *Review of particle physics*, *Phys. Rev. D* **110** (2024), no. 3 030001.
- [4] J. H. Christenson, J. W. Cronin, V. L. Fitch, and R. Turlay, *Evidence for the 2π Decay of the K_2^0 Meson*, *Phys. Rev. Lett.* **13** (1964) 138–140.
- [5] S. F. King, *Unified Models of Neutrinos, Flavour and CP Violation*, *Prog. Part. Nucl. Phys.* **94** (2017) 217–256, [[arXiv:1701.04413](#)].
- [6] Z.-z. Xing, *Flavor structures of charged fermions and massive neutrinos*, *Phys. Rept.* **854** (2020) 1–147, [[arXiv:1909.09610](#)].
- [7] F. Feruglio and A. Romanino, *Lepton flavor symmetries*, *Rev. Mod. Phys.* **93** (2021), no. 1 015007, [[arXiv:1912.06028](#)].
- [8] G.-J. Ding and J. W. F. Valle, *The symmetry approach to quark and lepton masses and mixing*, *Phys. Rept.* **1109** (2025) 1–105, [[arXiv:2402.16963](#)].
- [9] J. C. Pati and A. Salam, *Is Baryon Number Conserved?*, *Phys. Rev. Lett.* **31** (1973) 661–664.
- [10] J. C. Pati and A. Salam, *Lepton Number as the Fourth Color*, *Phys. Rev. D* **10** (1974) 275–289. [Erratum: *Phys. Rev. D* **11**, 703–703 (1975)].
- [11] H. Georgi and S. L. Glashow, *Unity of All Elementary Particle Forces*, *Phys. Rev. Lett.* **32** (1974) 438–441.
- [12] H. Georgi, H. R. Quinn, and S. Weinberg, *Hierarchy of Interactions in Unified Gauge Theories*, *Phys. Rev. Lett.* **33** (1974) 451–454.
- [13] H. Georgi, *The State of the Art—Gauge Theories*, *AIP Conf. Proc.* **23** (1975) 575–582.
- [14] H. Fritzsch and P. Minkowski, *Unified Interactions of Leptons and Hadrons*, *Annals Phys.* **93** (1975) 193–266.
- [15] **Super-Kamiokande** Collaboration, A. Takenaka et al., *Search for proton decay via $p \rightarrow e^+\pi^0$ and $p \rightarrow \mu^+\pi^0$ with an enlarged fiducial volume in Super-Kamiokande I-IV*, *Phys. Rev. D* **102** (2020), no. 11 112011, [[arXiv:2010.16098](#)].
- [16] N. Sakai, *Naturalness in Supersymmetric Guts*, *Z. Phys. C* **11** (1981) 153.
- [17] S. Dimopoulos and H. Georgi, *Softly Broken Supersymmetry and $SU(5)$* , *Nucl. Phys. B* **193** (1981) 150–162.
- [18] J. R. Ellis, S. Kelley, and D. V. Nanopoulos, *Probing the desert using gauge coupling unification*, *Phys. Lett. B* **260** (1991) 131–137.
- [19] U. Amaldi, W. de Boer, and H. Furstenau, *Comparison of grand unified theories with electroweak and strong coupling constants measured at LEP*, *Phys. Lett. B* **260** (1991) 447–455.
- [20] P. Langacker and M.-x. Luo, *Implications of precision electroweak experiments for M_t , p_0 , $\sin^2\theta_W$ and grand unification*, *Phys. Rev. D* **44** (1991) 817–822.
- [21] C. Giunti, C. W. Kim, and U. W. Lee, *Running coupling constants and grand unification models*, *Mod. Phys. Lett. A* **6** (1991) 1745–1755.
- [22] F. Feruglio, *Are neutrino masses modular forms?*, pp. 227–266. 2019. [[arXiv:1706.08749](#)].
- [23] S. Ferrara, D. Lust, A. D. Shapere, and S. Theisen, *Modular Invariance in Supersymmetric Field Theories*, *Phys. Lett. B* **225** (1989) 363.
- [24] E. J. Chun, J. Mas, J. Lauer, and H. P. Nilles, *Duality and Landau-ginzburg Models*, *Phys. Lett. B* **233** (1989) 141–146.
- [25] J. Lauer, J. Mas, and H. P. Nilles, *Twisted sector representations of discrete background symmetries for two-dimensional orbifolds*, *Nucl. Phys. B* **351** (1991) 353–424.

- [26] G. Altarelli and F. Feruglio, *Tri-bimaximal neutrino mixing, $A(4)$ and the modular symmetry*, *Nucl. Phys. B* **741** (2006) 215–235, [[hep-ph/0512103](#)].
- [27] C. Luhn, S. Nasri, and P. Ramond, *Tri-bimaximal neutrino mixing and the family symmetry semidirect product of $Z(7)$ and $Z(3)$* , *Phys. Lett. B* **652** (2007) 27–33, [[arXiv:0706.2341](#)].
- [28] C. Luhn, S. Nasri, and P. Ramond, *Simple Finite Non-Abelian Flavor Groups*, *J. Math. Phys.* **48** (2007) 123519, [[arXiv:0709.1447](#)].
- [29] R. de Adelhart Toorop, F. Feruglio, and C. Hagedorn, *Finite Modular Groups and Lepton Mixing*, *Nucl. Phys. B* **858** (2012) 437–467, [[arXiv:1112.1340](#)].
- [30] T. Kobayashi and M. Tanimoto, *Modular flavor symmetric models*, **7**, 2023. [[arXiv:2307.03384](#)].
- [31] G.-J. Ding and S. F. King, *Neutrino mass and mixing with modular symmetry*, *Rept. Prog. Phys.* **87** (2024), no. 8 084201, [[arXiv:2311.09282](#)].
- [32] B.-Y. Qu and G.-J. Ding, *Non-holomorphic modular flavor symmetry*, *JHEP* **08** (2024) 136, [[arXiv:2406.02527](#)].
- [33] G.-J. Ding, F. Feruglio, and X.-G. Liu, *Automorphic Forms and Fermion Masses*, *JHEP* **01** (2021) 037, [[arXiv:2010.07952](#)].
- [34] T. Nomura and H. Okada, *Type-II seesaw of a non-holomorphic modular A_4 symmetry*, [[arXiv:2408.01143](#)].
- [35] G.-J. Ding, J.-N. Lu, S. T. Petcov, and B.-Y. Qu, *Non-holomorphic modular S_4 lepton flavour models*, *JHEP* **01** (2025) 191, [[arXiv:2408.15988](#)].
- [36] C.-C. Li, J.-N. Lu, and G.-J. Ding, *Non-holomorphic modular A_5 symmetry for lepton masses and mixing*, *JHEP* **12** (2024) 189, [[arXiv:2410.24103](#)].
- [37] T. Nomura and H. Okada, *Zee model in a non-holomorphic modular A_4 symmetry*, [[arXiv:2412.18095](#)].
- [38] H. Okada and Y. Orikasa, *A radiative seesaw in a non-holomorphic modular S_3 flavor symmetry*, [[arXiv:2501.15748](#)].
- [39] T. Kobayashi, H. Okada, and Y. Orikasa, *Zee-Babu model in a non-holomorphic modular A_4 symmetry and modular stabilization*, [[arXiv:2502.12662](#)].
- [40] H. Ishimori, Y. Shimizu, and M. Tanimoto, *$S(4)$ Flavor Symmetry of Quarks and Leptons in $SU(5)$ GUT*, *Prog. Theor. Phys.* **121** (2009) 769–787, [[arXiv:0812.5031](#)].
- [41] C. Hagedorn, S. F. King, and C. Luhn, *A $SUSY$ GUT of Flavour with $S_4 \times SU(5)$ to NLO*, *JHEP* **06** (2010) 048, [[arXiv:1003.4249](#)].
- [42] C. Hagedorn, S. F. King, and C. Luhn, *$SUSY S_4 \times SU(5)$ revisited*, *Phys. Lett. B* **717** (2012) 207–213, [[arXiv:1205.3114](#)].
- [43] M. Dimou, S. F. King, and C. Luhn, *Approaching Minimal Flavour Violation from an $SU(5) \times S_4 \times U(1)$ $SUSY$ GUT*, *JHEP* **02** (2016) 118, [[arXiv:1511.07886](#)].
- [44] M. Dimou, S. F. King, and C. Luhn, *Phenomenological implications of an $SU(5) \times S_4 \times U(1)$ $SUSY$ GUT of flavor*, *Phys. Rev. D* **93** (2016), no. 7 075026, [[arXiv:1512.09063](#)].
- [45] G. Altarelli, F. Feruglio, and C. Hagedorn, *A $SUSY SU(5)$ Grand Unified Model of Tri-Bimaximal Mixing from A_4* , *JHEP* **03** (2008) 052, [[arXiv:0802.0090](#)].
- [46] P. Ciafaloni, M. Picariello, E. Torrente-Lujan, and A. Urbano, *Neutrino masses and tribimaximal mixing in Minimal renormalizable $SUSY SU(5)$ Grand Unified Model with $A(4)$ Flavor symmetry*, *Phys. Rev. D* **79** (2009) 116010, [[arXiv:0901.2236](#)].
- [47] P. Ciafaloni, M. Picariello, A. Urbano, and E. Torrente-Lujan, *Toward minimal renormalizable $SUSY SU(5)$ Grand Unified Model with tribimaximal mixing from $A(4)$ Flavor symmetry*, *Phys. Rev. D* **81** (2010) 016004, [[arXiv:0909.2553](#)].
- [48] I. K. Cooper, S. F. King, and C. Luhn, *$SUSY SU(5)$ with singlet plus adjoint matter and A_4 family symmetry*, *Phys. Lett. B* **690** (2010) 396–402, [[arXiv:1004.3243](#)].
- [49] I. K. Cooper, S. F. King, and C. Luhn, *$A_4 \times SU(5)$ $SUSY$ GUT of Flavour with Trimaximal Neutrino Mixing*, *JHEP* **06** (2012) 130, [[arXiv:1203.1324](#)].
- [50] F. Björkeroth, F. J. de Anda, I. de Medeiros Varzielas, and S. F. King, *Towards a complete $A_4 \times SU(5)$ $SUSY$ GUT*, *JHEP* **06** (2015) 141, [[arXiv:1503.03306](#)].
- [51] R. A. Laamara, M. A. Loualidi, M. Miskaoui, and E. H. Saidi, *Hybrid seesaw neutrino model in $SUSY SU(5) \times A_4$* , *Phys. Rev. D* **98** (2018), no. 1 015004, [[arXiv:1806.08573](#)].
- [52] L. O. E. Ramos, M. Mondragón, G. Patellis, and G. Zoupanos, *Flavor in $SU(5)$ Finite Grand Unified Models*, *Fortsch. Phys.* **72** (2024), no. 12 2400177, [[arXiv:2406.17702](#)].
- [53] R. Ahl Laamara, M. A. Loualidi, M. Miskaoui, and E. H. Saidi, *Fermion masses and mixing in $SU(5) \times D_4 \times U(1)$ model*, *Nucl. Phys. B* **916** (2017) 430–462.
- [54] M. Miskaoui and M. A. Loualidi, *Leptogenesis, fermion masses and mixings in a $SUSY SU(5)$ GUT with D_4 flavor symmetry*, *JHEP* **11** (2021) 147, [[arXiv:2106.07332](#)].
- [55] M. A. Loualidi and M. Miskaoui, *Unflavored Leptogenesis and Neutrino Masses in Flavored $SUSY SU(5)$ model*, in *1st Pan-African Astro-Particle and Collider Physics Workshop*, **6**, 2022. [[arXiv:2206.01052](#)].
- [56] G.-J. Ding, S. F. King, and C.-Y. Yao, *Modular $S_4 \times SU(5)$ GUT*, *Phys. Rev. D* **104** (2021), no. 5 055034, [[arXiv:2103.16311](#)].
- [57] S. F. King and Y.-L. Zhou, *Twin modular S_4 with $SU(5)$ GUT*, *JHEP* **04** (2021) 291, [[arXiv:2103.02633](#)].
- [58] I. de Medeiros Varzielas, S. F. King, and M. Levy, *A modular $SU(5)$ littlest seesaw*, *JHEP* **05** (2024) 203, [[arXiv:2309.15901](#)].
- [59] F. J. de Anda, S. F. King, and E. Perdomo, *$SU(5)$ grand unified theory with A_4 modular symmetry*, *Phys. Rev. D* **101** (2020), no. 1 015028, [[arXiv:1812.05620](#)].
- [60] P. Chen, G.-J. Ding, and S. F. King, *$SU(5)$ GUTs with A_4 modular symmetry*, *JHEP* **04** (2021) 239, [[arXiv:2101.12724](#)].
- [61] T. Kobayashi, Y. Shimizu, K. Takagi, M. Tanimoto, and T. H. Tatsuishi, *Modular S_3 -invariant flavor model in $SU(5)$*

- grand unified theory*, *PTEP* **2020** (2020), no. 5 053B05, [arXiv:1906.10341].
- [62] X. Du and F. Wang, *SUSY breaking constraints on modular flavor S_3 invariant $SU(5)$ GUT model*, *JHEP* **02** (2021) 221, [arXiv:2012.01397].
 - [63] P. Minkowski, $\mu \rightarrow e\gamma$ at a Rate of One Out of 10^9 Muon Decays?, *Phys. Lett. B* **67** (1977) 421–428.
 - [64] T. Yanagida, *Proc. workshop on unified theory and the baryon number in the universe*, KEK Report No. 79-18 **95** (1979).
 - [65] M. Gell-Mann, P. Ramond, and R. Slansky, *Complex Spinors and Unified Theories*, *Conf. Proc. C* **790927** (1979) 315–321, [arXiv:1306.4669].
 - [66] S. L. Glashow, *The Future of Elementary Particle Physics*, NATO Sci. Ser. B **61** (1980) 687.
 - [67] R. N. Mohapatra and G. Senjanovic, *Neutrino Mass and Spontaneous Parity Nonconservation*, *Phys. Rev. Lett.* **44** (1980) 912.
 - [68] X.-G. Liu and G.-J. Ding, *Neutrino Masses and Mixing from Double Covering of Finite Modular Groups*, *JHEP* **08** (2019) 134, [arXiv:1907.01488].
 - [69] A. Borel, *Automorphic forms on reductive groups*, *Automorphic forms and applications*, IAS/Park City mathematics series **12** (2007) 5–40.
 - [70] A. Borel, *Algebraic groups and discontinuous subgroups*, in *Proc. Sympos. Pure Math.*, Amer. Math. Soc., Providence, 1966.
 - [71] J. C. Lagarias and R. C. Rhoades, *Polyharmonic maass forms for $psl(2, z)$* , *The Ramanujan Journal* **41** (2016) 191–232.
 - [72] H. Georgi and C. Jarlskog, *A New Lepton - Quark Mass Relation in a Unified Theory*, *Phys. Lett. B* **86** (1979) 297–300.
 - [73] K. S. Babu, B. Bajc, and S. Saad, *Yukawa Sector of Minimal $SO(10)$ Unification*, *JHEP* **02** (2017) 136, [arXiv:1612.04329].
 - [74] I. Esteban, M. C. Gonzalez-Garcia, M. Maltoni, I. Martinez-Soler, J. a. P. Pinheiro, and T. Schwetz, *NuFit-6.0: updated global analysis of three-flavor neutrino oscillations*, *JHEP* **12** (2024) 216, [arXiv:2410.05380].
 - [75] **Planck** Collaboration, N. Aghanim et al., *Planck 2018 results. VI. Cosmological parameters*, *Astron. Astrophys.* **641** (2020) A6, [arXiv:1807.06209]. [Erratum: *Astron. Astrophys.* 652, C4 (2021)].
 - [76] **KamLAND-Zen** Collaboration, S. Abe et al., *Search for Majorana Neutrinos with the Complete KamLAND-Zen Dataset*, arXiv:2406.11438.
 - [77] **LEGEND** Collaboration, N. Abgrall et al., *The Large Enriched Germanium Experiment for Neutrinoless $\beta\beta$ Decay: LEGEND-1000 Preconceptual Design Report*, arXiv:2107.11462.
 - [78] **nEXO** Collaboration, G. Adhikari et al., *nEXO: neutrinoless double beta decay search beyond 10^{28} year half-life sensitivity*, *J. Phys. G* **49** (2022), no. 1 015104, [arXiv:2106.16243].
 - [79] **Katrin** Collaboration, M. Aker et al., *Direct neutrino-mass measurement based on 259 days of KATRIN data*, arXiv:2406.13516.
 - [80] **KATRIN** Collaboration, M. Aker et al., *The design, construction, and commissioning of the KATRIN experiment*, *JINST* **16** (2021), no. 08 T08015, [arXiv:2103.04755].
 - [81] A. Baur, *FlavorPy*, 2024.
 - [82] M. Belfkir, M. A. Lualidi, and S. Nasri, *Fermion Masses and Mixing in Pati-Salam Unification with S_3 Modular Symmetry*, arXiv:2501.00302.
 - [83] **Project 8** Collaboration, A. Ashtari Esfahani et al., *Determining the neutrino mass with cyclotron radiation emission spectroscopy—Project 8*, *J. Phys. G* **44** (2017), no. 5 054004, [arXiv:1703.02037].
 - [84] T. Goto, S. Mishima, and T. Shindou, *Flavor physics in $SU(5)$ GUT with scalar fields in the 45 representation*, *Phys. Rev. D* **108** (2023), no. 9 095012, [arXiv:2308.13329].
 - [85] N. Haba, K. Nagano, Y. Shimizu, and T. Yamada, *Gauge Coupling Unification and Proton Decay via 45 Higgs Boson in $SU(5)$ GUT*, *PTEP* **2024** (2024), no. 5 053B05, [arXiv:2402.15124].
 - [86] N. Haba, K. Nagano, Y. Shimizu, and T. Yamada, *Proton Decay and Gauge Coupling Unification in an Extended $SU(5)$ GUT with 45D Higgs*, *PTEP* **2024** (2024), no. 10 103B04, [arXiv:2406.11091].
 - [87] P. Nath and P. Fileviez Perez, *Proton stability in grand unified theories, in strings and in branes*, *Phys. Rept.* **441** (2007) 191–317, [hep-ph/0601023].
 - [88] I. Dorsner, S. Fajfer, and N. Kosnik, *Heavy and light scalar leptoquarks in proton decay*, *Phys. Rev. D* **86** (2012) 015013, [arXiv:1204.0674].
 - [89] I. Dorsner, *A scalar leptoquark in $SU(5)$* , *Phys. Rev. D* **86** (2012) 055009, [arXiv:1206.5998].
 - [90] **CMS** Collaboration, V. Khachatryan et al., *Search for narrow resonances decaying to dijets in proton-proton collisions at $\sqrt{s} = 13$ TeV*, *Phys. Rev. Lett.* **116** (2016), no. 7 071801, [arXiv:1512.01224].
 - [91] R. Ahl Laamara, M. A. Lualidi, and E. H. Saidi, *Type II seesaw supersymmetric neutrino model for $\theta_{13} \neq 0$* , *Phys. Rev. D* **93** (2016), no. 11 113005, [arXiv:1606.04788].
 - [92] M. A. Ouahid, M. A. Lualidi, R. A. Laamara, and E. H. Saidi, *Neutrino phenomenology in the flavored NMSSM without domain wall problems*, *Phys. Rev. D* **102** (2020), no. 11 115023, [arXiv:1810.10753].